obtained after excitation by high intensity and for a long time, at least for ZnS:[Zn]:Cu phosphors, are not affected by retrapping.

The existence of a series of discrete trap depths, at least 12 in number between $-100°$ and 200°C, appears plausible. Definite evidence, however, was not obtained that a continuous distribution of trap depths, followed by one or two discrete depths, could not give an alternative description of the observed results.

A study of the crystal structure of ZnS indicates that interstitial positions are all different in cubic and hexagonal ZnS, whereas substitutional positions are the same out to third nearest neighbors. A new analytical approach was indicated, therefore, which states that, if formation of simple defects does not alter symmetry relations, luminescence phenomena caused by impurities in interstitial positions should be different when observed in cubic and hexagonal ZnS phosphors, but that luminescence phenomena caused by impurities in substitutional positions should be the same or practically the same when observed in cubic and hexagonal ZnS phosphors.

The similarity in trap depths found for cubic and hexagonal phosphors leads to the hypothesis that trapping centers are located in substitutional sites, primarily omission defects. This hypothesis and the previously mentioned analytical approach may be used to interpret many observations of luminescence emission and glow curves.

The author wishes to express his sincere appreciation to H. W. Leverenz and Dr. R. E. Shrader for many valuable discussions, suggestions, and encouragement throughout the work; to Professor R. Hofstadter[31] of Princeton University for his capable advice and guidance; and to the entire staff of the Chemico-Physics section at the RCA Laboratories for the assistance they gladly and skillfully contributed at various phases of the work.

The author also wishes to thank Dr. V. K. Zworykin of the Radio Corporation of America, and the ONR for enabling a concentrated program of this type to be carried out.

[31] Present address: Physics Dept., Stanford University.

PHYSICAL REVIEW VOLUME 80, NUMBER 4 NOVEMBER 15, 1950

Quantum Electrodynamics of Charged Particles without Spin

F. ROHRLICH
Laboratory of Nuclear Studies, Cornell University, Ithaca, New York

(Received June 19, 1950)

Feynman's formulation of quantum electrodynamics is shown to be equivalent to the Schwinger-Tomonaga theory also for spinless charged particles (mesons) as developed by Kanesawa and Tomonaga. The divergencies of the scattering matrix are analyzed to all orders in the fine-structure constant and it is found that mass and charge renormalizations do *not* remove all divergencies, unlike the electron case. The remaining divergence is associated with the meson-meson interaction and occurs in all orders of radiative corrections except the lowest (second) order in which the process can exist. In order to make the scattering matrix completely finite a direct interaction term $\lambda\phi^*(x)\phi^*(x)\phi(x)\phi(x)$ in the Hamiltonian must be postulated. The infinite coupling constant λ is to be renormalized by an infinite renormalization. One obtains a finite amount of direct interation which must be determined from experiment. The identical cancellation of certain divergencies to all orders of the fine-structure constant and valid for spin 0, $\frac{1}{2}$, and 1 is proven in the Appendix.

I. INTRODUCTION

THE theory of the interaction of elementary particles has been formulated in two equivalent ways by Schwinger and Tomonaga, and by Feynman. So far the equivalence has been proven explicitly only for the interaction of electrons with the electromagnetic field,[1] but there seems to be little doubt that it holds also for the interaction of the electromagnetic field with particles of other spin and for nuclear interactions as described by meson theories. Also, a consistent separation and removal of divergencies to all orders in the coupling constant has so far been shown possible only for the quantum electrodynamics of the electron. Dyson[2] showed that this could be achieved by a consistent procedure of mass and charge renormalization. The resultant finite effects as far as they have been calculated seem to agree well with experiments. This theory is therefore outstanding as the only one both as to finiteness to all orders and correctness.[3]

This success of the theory of the interaction of electrons, positrons, and photons warrants a similar investigation for other elementary particles. As a first step

[1] F. J. Dyson, Phys. Rev. 75, 486 (1949). In the following quoted as I.

[2] F. J. Dyson, Phys. Rev. 75, 1736 (1949). In the following quoted as II.

[3] For an extension of these results to the interaction of spinless mesons with nucleons see P. T. Matthews, Phil. Mag. 41, 185 (1950) and Phys. Rev. (to be published).

in this direction the interaction of positively and negatively charged spinless mesons with the electromagnetic field is considered in this paper.

We first show the equivalence of the Schwinger-Tomonaga theory[4] and the Feynman theory[5] for this case. In Section III a sufficient condition for the finiteness of the number of primitive divergencies of the scattering matrix is derived. These divergencies are enumerated and the unexpected divergence of meson-meson interaction is found. All divergencies are then separated from the finite observable parts of the S matrix and are removed by renormalization (Section IV). For this purpose a direct meson-meson interaction must be introduced whose coupling constant must be renormalized together with the mass and charge of the mesons. A finite and unambiguous S matrix is obtained. Section V deals with the explicit calculation of the infinite parts of some primitive divergent processes to lowest order. In Section VI the results are summarized and the determination of the coupling constant of direct interaction from experiment is discussed. The two appendices prove the cancellation of spurious charge and wave function renormalization and show the asymptotic behavior of the finite parts of primitive divergent processes.

II. EQUIVALENCE OF THE THEORIES OF FEYNMAN AND KANESAWA-TOMONAGA

Let $\phi(x)$ and $A_\mu(x)$ denote the meson field and the electromagnetic field. The interaction of the two fields will be given by the Tomonaga-Schwinger equation[6]

$$i\delta\Psi[\sigma]/\delta\sigma(x)=\mathcal{H}[x]\Psi[\sigma], \tag{1}$$

where

$$\mathcal{H}[x]=ieA_\mu(\phi^*\partial_\mu\phi-(\partial_\mu\phi^*)\phi)+e^2\phi^*\phi(A_\mu A_\mu+(n_\mu A_\mu)^2) \tag{2}$$

is the Hamiltonian in the interaction representation. This Hamiltonian is obtained from the Heisenberg representation by a unitary transformation and fulfills the integrability condition

$$\delta^2\Psi[\sigma]/\delta\sigma(x)\delta\sigma(x')=\delta^2\Psi[\sigma]/\delta\sigma(x')\delta\sigma(x)$$

or

$$[\mathcal{H}[x],\mathcal{H}[x']]=i\frac{\delta\mathcal{H}[x']}{\delta\sigma(x)}-i\frac{\delta\mathcal{H}[x]}{\delta\sigma(x')}. \tag{3}$$

As can be seen by generalizing the Hamiltonian for a flat surface to one for a space-like surface, Eq. (3) leads to the introduction of normal-dependent terms only for derivative coupling. These terms therefore occur for bosons but not for electrons.

The formal solution of (1) is

$$\Psi[\sigma]=S[\sigma,\sigma_0]\Psi[\sigma_0], \tag{4}$$

which expresses the state of the system on the space-like surface σ in terms of the given state on σ_0. The "propagation matrix"

$$S[\sigma,\sigma_0]=1+(-i)\int_{\sigma_0}^{\sigma}\mathcal{H}[x^1]d_4x'+(-i)^2\int_{\sigma_0}^{\sigma}dx^1\int_{\sigma_0}^{\sigma(x')}\mathcal{H}[x^1]\mathcal{H}[x^2]d_4x^2+\cdots$$

can be symmetrized in the time coordinates of the intermediate states to give (see Dyson **I**)

$$S[\sigma,\sigma_0]=1+\sum_{n=1}^{\infty}((-i)^n/n!)\int_{\sigma_0}^{\sigma}P\left(\prod_{k=1}^{n}\mathcal{H}[x^k]d_4x^k\right). \tag{5}$$

P denotes the ordering operator in time: The factors $\mathcal{H}[x^1],\cdots\mathcal{H}[x^n]$ are to be arranged in increasing (decreasing) order of the parameter labeling the family of space-like surfaces between σ_0 and σ when read from right to left and the integration extends from σ_0 to the later (earlier) surface σ. $S[\sigma,\sigma_0]$ is symmetrical in past and future and is unitary. It follows from the Hermitian property of $\mathcal{H}[x]$ that

$$\begin{aligned}S^{-1}[\sigma,\sigma_0]&=S^\dagger[\sigma,\sigma_0]\\&=1+\sum_{n=1}^{\infty}(i^n/n!)\int_{\sigma_0}^{\sigma}P^{-1}\left(\prod_{k=1}^{n}\mathcal{H}[x^k]d_4x^k\right)\\&=1+\sum_{n=1}^{\infty}((-i)^n/n!)\int_{\sigma}^{\sigma_0}P\left(\prod_{k=1}^{n}\mathcal{H}[x^k]d_4x^k\right)\\&=S[\sigma_0,\sigma].\end{aligned} \tag{6}$$

P^{-1} denotes the ordering operator which arranges the factors in opposite order to P. Equation (6) is consistent with the propagation property of $S[\sigma,\sigma_0]$,

$$S[\sigma,\sigma_0]=S[\sigma,\sigma_1]S[\sigma_1,\sigma_0], \tag{7}$$

$$S[\sigma_0,\sigma_0]=1. \tag{7'}$$

The propagation matrix satisfies the equations

$$i\delta S[\sigma,\sigma_0]/\delta\sigma(x)=\mathcal{H}[x]S[\sigma,\sigma_0], \tag{8a}$$

$$i\delta S[\sigma,\sigma_0]/\delta\sigma(x^0)=-S[\sigma,\sigma_0]\mathcal{H}[x^0]. \tag{8b}$$

These equations are equivalent to (5), (6), and (7). As a special case of the propagation matrix we obtain the

[4] The Schwinger-Tomonaga theory was first applied to the electromagnetic interaction of spinless mesons by S. Kanesawa and S. Tomonaga, Prog. Theor. Phys. **3**, 1 (1948). For a treatment with Kemmer-Duffin matrices see M. Neuman and W. H. Furry, Phys. Rev. **76**, 1677 (1949); R. G. Moorhouse, Phys. Rev. **76**, 1691 (1949).

[5] R. P. Feynman, Phys. Rev. **76**, 749, 769 (1949).

[6] Throughout this paper we use the units $\hbar=c=1$. $\partial_\mu=\partial/\partial x_\mu$. Otherwise we use the same notation as Schwinger with $x\equiv(x_1,x_2,x_3,x_4=ix_0)$ and $d_4x=dx_1dx_2dx_3dx_0$. In particular a square bracket surrounding an argument indicates a functional, and we use Heaviside-Lorentz units.

scattering matrix

$$S=S[\infty,-\infty]$$
$$=1+\sum_{n=1}^{\infty}((-i)^n/n!)\int_{-\infty}^{\infty}P\left(\prod_{k=1}^{n}\mathcal{H}[x^k]d_4x^k\right) \quad (5')$$

as given in **I**.

The non-linearity in the electromagnetic field of the interaction Hamiltonian for spinless mesons as compared to the interaction Hamiltonian for electrons is of great importance; the Compton effect to lowest order will be partially due to a direct interaction. If an unquantized external electromagnetic field is acting on the system, its potential $A_\mu^e(x)$ will superimpose linearly on the radiation field potential $A_\mu(x)$. The resulting interaction Hamiltonian

$$\mathcal{H}^i[x]=ie(A_\mu+A_\mu^e)(\phi^*\partial_\mu\phi-(\partial_\mu\phi^*)\phi)$$
$$+e^2\phi^*\phi[(A_\mu+A_\mu^e)(A_\mu+A_\mu^e)+[n_\mu(A_\mu+A_\mu^e)]^2] \quad (9)$$

cannot be written as the sum of the interaction Hamiltonians with the radiation field and with the external field, but it will contain a cross term $\mathcal{H}^c[x]$

$$\mathcal{H}^i[x]=\mathcal{H}[x]+\mathcal{H}^c[x]+\mathcal{H}^e[x], \quad (9')$$

$$\mathcal{H}^c[x]=2e^2\phi^*\phi(A_\mu A_\mu^e+n_\mu A_\mu n_\nu A_\nu^e). \quad (10)$$

$\mathcal{H}[x]$ describes the interaction of the mesons with their own radiation field and with photons in the absence of an external field, as given by Eq. (2). $\mathcal{H}^e[x]$ is defined as (2) with A_μ replaced by A_μ^e. It is the interaction of the mesons with the external field in the absence of a quantized electromagnetic field (no radiative corrections and no photons present). The cross term, $\mathcal{H}^c[x]$, permits the mesons to emit or absorb a photon under the simultaneous action of an external field. The fundamental Eq. (1) now becomes

$$i\delta\Psi[\sigma]/\delta\sigma(x)=\mathcal{H}^i[x]\Psi[\sigma] \quad (1')$$

and yields as before the scattering matrix

$$S=1+\sum_{n=1}^{\infty}((-i)^n/n!)\int_{-\infty}^{\infty}P\left(\prod_{k=1}^{n}\mathcal{H}^i[x^k]d_4x^k\right) \quad (11)$$

of which (5′) is a special case.

If one restricts himself to the problem of a single charged particle interacting with an external electromagnetic field taking account of radiative corrections, it is possible to obtain an effective interaction Hamiltonian to lowest order in the external field by a unitary transformation which eliminates the explicit appearance of the virtual radiation field. In the electron case, the effective Hamiltonian of this special problem lends itself to a simple physical interpretation which gives a link between the physical pictures underlying the Tomonaga-Schwinger and the Feynman theory. A similar transformation can be carried out in the case of integral spin, but due to the non-linearity in the electromagnetic field as manifested in the cross term (10), this transformation will depend on the external field.[7] The effective Hamiltonian thus constructed is not any simple physically meaningful quantity even in the special case considered. On the other hand, the S matrix (11) is perfectly general and does constitute the main link between the two theories, both in its physical meaning and in its mathematical character.

In evaluating the S matrix one takes the expectation value in occupation number space of the operator (11), corresponding to the number of mesons and photons emitted and absorbed, and inserts the external field of the particular problem under consideration. $S(\sigma,\sigma_0)$ then expresses the probability amplitude for a system of mesons and photons as given on σ_0 to arrive on σ in a specified way after interaction with the given external field. This includes in general all radiative corrections.

The physical idea underlying the Feynman theory is to follow one possible world line of each participating particle from the initial to the final space-time point during which time the particles interact with each other and with the external field. One constructs the probability amplitude for this case by a specified procedure from the "propagation functions" for the individual particles, and then sums over all possible world lines between the two space-time points. The propagation functions are related to the particles in a similar way as the propagation matrix $S(\sigma,\sigma_0)$ is related to the whole system. They are the probability amplitudes for arrival at a specified space-time point for a particle that started out at an other given space-time point; their propagation property is manifested by an equation similar to Eq. (7) (cf. Feynman[5]). It follows that the resultant integral has the same physical interpretation as does the S matrix. In the remainder of this section we shall show that it is also mathematically identical with the scattering matrix (11). This will be done by deriving from (11) the Feynman procedure for the construction of the S matrix.

We assume first that no external field is acting ($A_\mu^e=0$). The S matrix is given by (5′). The general problem to be solved will be to find the radiative corrections of order n' (an even number) for a system

[7] It would seem at first that the use of the Kemmer-Duffin matrices, β_μ, may not lead to a cross term since the equations of motion in the Heisenberg representation are linear in the electromagnetic field. However, in the interaction representation the Hamiltonian contains the quadratic terms

$$(e^2/m)(\bar\psi\beta_\mu\beta_\nu\psi+\bar\psi\beta_\mu(n_\lambda\beta_\lambda)^2\beta_\nu\psi)A_\mu A_\nu$$

(see Newmann and Furry, and Moorhouse, reference 4), of which only the second, normal-dependent term can be ignored, since it cancels out in the S matrix. Therefore, the interaction with an external field leads to a cross term also here. Note, however, that the Kemmer-Duffin matrices do permit one to write the S matrix formally as if the interaction were linear in the field, such that only single-corner diagrams need to be considered. Notwithstanding this advantage we have preferred not to use the Kemmer-Duffin matrices in this paper, because their singular character partially overestimates the divergencies of the S matrix.

involving the interaction of m mesons[8] and p photons. All terms in (5′) with

$$p+n'\geqslant n\geqslant\begin{cases}(p+n')/2, & p \text{ even}\\(p+n'+1)/2, & p \text{ odd}\end{cases}$$

will contribute. $n'+p$ is the power to which the electric charge e occurs; n is the number of Hamiltonians in the integrand and is equal to the number of four-vectors $x_\mu{}^k$ ($k=1, 2, \cdots n$) over which the integration is carried out. For each value of n the integrand will contain terms of all orders between e^n and e^{2n}. Only the term of order $e^{n'+p}$ will contribute in our problem. This term will be a sum of P brackets, each being a product of $2n-n'-p$ factors A_μ, $n'+p-n$ factors $A_\mu A_\mu+(n_\mu A_\mu)^2$, $n+p$ factors ϕ^*, and $n+p$ factors ϕ; the latter two will sometimes be preceded by a differentiation operator. From each product we now select p operators A_μ corresponding to the emission and/or absorption of p photons, m operators ϕ, each for either a positive ingoing or a negative outgoing meson, and m operators ϕ^*, each for either a negative ingoing or a positive outgoing meson. The remaining operators ϕ and ϕ^*, possibly preceded by a differentiation operator, will combine in pairs $\phi(x^i)\phi^*(x^k)$ to give vacuum expectation values; similarly, the remaining factors A_μ have to combine in pairs to give vacuum expectation values. In order to make this possible n' has to be even as mentioned previously. Since each pair of operators refers to a different particle, the P bracket will break up into P brackets of pairs, and one obtains the following vacuum expectation values of P brackets:

$$\langle P(A_\mu(x^i), A_\nu(x^k))\rangle_0=\tfrac{1}{2}\delta_{\mu\nu}D_F(x^i-x^k), \qquad (12)$$

$$\langle P(\phi(x^i), \phi^*(x^k))\rangle_0=\tfrac{1}{2}\Delta_F(x^i-x^k), \qquad (13)$$

$$\begin{aligned}&\langle P(\partial_\mu{}^{(i)}\phi(x^i), \phi^*(x^k))\rangle_0\\&=\tfrac{1}{2}\partial_\mu{}^{(i)}\Delta^{(1)}(x^i-x^k)+\tfrac{1}{2}i\epsilon(x^i, x^k)\partial_\mu{}^{(i)}\Delta(x^i-x^k)\\&=\tfrac{1}{2}\partial_\mu{}^{(i)}\Delta_F(x^i-x^k)-\tfrac{1}{2}i\Delta(x^i-x^k)\partial_\mu{}^{(i)}\epsilon(x^i, x^k), \qquad (14a)\end{aligned}$$

$$\begin{aligned}&\langle P(\phi(x^i), \partial_\mu{}^{(k)}\phi^*(x^k))\rangle_0\\&=\tfrac{1}{2}\partial_\mu{}^{(k)}\Delta_F(x^i-x^k)-\tfrac{1}{2}\Delta(x^i-x^k)\partial_\mu{}^{(k)}\epsilon(x^i, x^k), \qquad (14b)\end{aligned}$$

$$\begin{aligned}&\langle P(\partial_\mu{}^{(i)}\phi(x^i)\partial_\nu{}^{(k)}\phi^*(x^k))\rangle_0\\&=\tfrac{1}{2}\partial_\mu{}^{(i)}\partial_\nu{}^{(k)}\Delta^{(1)}(x^i-x^k)\\&\qquad+\tfrac{1}{2}i\epsilon(x^i, x^k)\partial_\mu{}^{(i)}\partial_\nu{}^{(k)}\Delta(x^i-x^k)\\&=\tfrac{1}{2}\partial_\mu{}^{(i)}\partial_\nu{}^{(k)}\Delta_F(x^i-x^k)\\&\quad-\tfrac{1}{2}i(\partial_\mu{}^{(i)}\epsilon(x^i, x^k))(\partial_\nu{}^{(k)}\Delta(x^i-x^k))\\&\qquad-\tfrac{1}{2}i\partial_\mu{}^{(i)}(\Delta(x^i-x^k)\partial_\nu{}^{(k)}\epsilon(x^i, x^k)). \qquad (15)\end{aligned}$$

These equations are a direct consequence of the definition of P

$$P(A(x^i), B(x^k))=\tfrac{1}{2}\{A(x^i), B(x^k)\}+\tfrac{1}{2}\epsilon(x^i, x^k)[A(x^i), B(x^k)]$$

(the brackets { } and [ ] denote the anticommutator and the commutator, and $\epsilon(x^i, x^k)=1$ or -1 for $\sigma(x^i)$ later or earlier than $\sigma(x^k)$), of the commutation relations

$$[A_\mu(x^i), A_\nu(x^k)]=i\delta_{\mu\nu}D(x^i-x^k), \qquad (16)$$

$$[\phi^*(x^i), \phi(x^k)]=i\Delta(x^i-x^k), \qquad (17)$$

and of the vacuum expectation values

$$\langle\{A_\mu(x^i), A_\nu(x^k)\}\rangle_0=\delta_{\mu\nu}D^{(1)}(x^i-x^k), \qquad (18)$$

$$\langle\{\phi^*(x^i), \phi(x^k)\}\rangle_0=\Delta^{(1)}(x^i-x^k). \qquad (19)$$

The functions D, $D^{(1)}$, Δ, and $\Delta^{(1)}$ are defined as in Schwinger's papers,[9] the functions D_F and Δ_F as in **I**. The relation between them is

$$D_F=D^{(1)}+i\epsilon D, \qquad (20a)$$

$$\Delta_F=\Delta^{(1)}+i\epsilon\Delta. \qquad (20b)$$

One now observes that,

$$\Delta(x^i-x^k)\partial_\mu{}^{(i)}\epsilon(x^i, x^k)=-2\Delta(x^i-x^k)n_\mu\delta(n_\lambda(x_\lambda{}^i-x_\lambda{}^k))=0$$

and that,

$$\begin{aligned}&(\partial_\mu{}^{(i)}\Delta(x^i-x^k))\partial_\nu{}^{(k)}\epsilon(x^i, x^k)\\&=n_\mu\delta(x_\lambda{}^i-x_\lambda{}^k+n_\lambda n_\sigma(x_\sigma{}^i-x_\sigma{}^k))2n_\nu\delta((x_\lambda{}^i-x_\lambda{}^k)n_\lambda)\\&=2n_\mu n_\nu\delta(x^i-x^k).\end{aligned}$$

The first expression vanishes because the δ-function of the time-like vector $n_\lambda(x_\lambda{}^i-x_\lambda{}^k)$ restricts the argument of the Δ-function to space-like vectors. As can be seen from Eq. (17), the Δ-function of space-like argument vanishes, since two operators of space-like separation commute. Therefore, the second term on the right side of Eqs. (14a) and (14b) vanishes, and (15) becomes

$$\begin{aligned}&\langle P(\partial_\mu{}^{(i)}\phi(x^i)\partial_\nu{}^{(k)}\phi^*(x^k))\rangle_0\\&=\tfrac{1}{2}\partial_\mu{}^{(i)}\partial_\nu{}^{(k)}\Delta_F(x^i-x^k)-in_\mu n_\nu\delta(x^i-x^k). \qquad (15')\end{aligned}$$

Consider first only the P brackets arising from the meson field, such that for a particular value of n we will have $2n-n'-p$ factors A_μ and $n'+p-n$ factors $A_\mu A_\mu+(n_\mu A_\mu)^2$, as mentioned above. Let one of the latter factors have the argument x^i. Clearly, this argument can be chosen in n different ways, since there are n dummy variables. There will therefore be a normal-dependent term in the integrand containing the factor

$$((-i)^n/n!)ne^2\phi^*(x^i)\phi(x^i)(n_\lambda A_\lambda(x^i))^2. \qquad (21)$$

[8] Any annihilated or created meson pair is counted here as one meson.

[9] J. S. Schwinger, Phys. Rev. **74**, 1439 (1948); **75**, 651 (1949); **76**, 790 (1949).

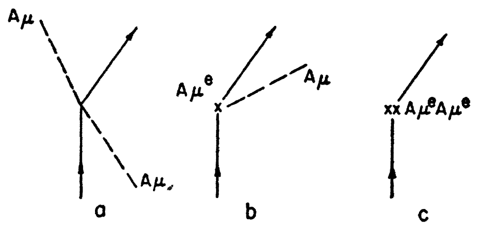

FIG. 1. Examples of double corners.

Such a term would not arise for $n=n'+p$; for $n<n'+p$ there exists a contribution of the same order n' from the $(n+1)$st term in (11). This term will contain $(2n+2-n'-p)$ factors A_μ and $(n'+p-n-1)$ factors $A_\mu A_\mu+(n_\mu A_\mu)^2$. It will therefore differ from the nth term by an additional factor $(-i)/(n+1)$ in front, by one additional integration over the one additional variable, and by two factors linear in A_μ instead of one factor quadratic in A_μ. These two linear factors may be given the arguments x^i and x^k in $(n+1)!/2!(n-1)!$ ways. Thus the $(n+1)$st term yields instead of (21)

$$\begin{aligned}&[(-i)^{n+1}/(n+1)!][(n+1)!/2!(n-1)!]ieA_\mu(x^i)\\&\quad\times(\phi^*(x^i)\partial_\mu{}^{(i)}\phi(x^i)-(\partial_\mu{}^{(i)}\phi^*(x^i))\phi(x^i))\\&\quad\times\int ieA_\nu(x^k)(\phi^*(x^k)\partial_\nu{}^{(k)}\phi(x^k)\\&\qquad\qquad-(\partial_\nu{}^{(k)}\phi^*(x^k))\phi(x^k))d_4x^k.\qquad(22)\end{aligned}$$

Since (22) contains one pair $\phi^*\phi$ more than does (21), it will give rise to one P bracket more. From (13), (14), and (15′) it is seen that only the terms in (22) involving two derivatives lead to normal-dependent terms; these are with the help of (15′)

$$\begin{aligned}&[(-i)^{n+1}/(n+1)!][(n+1)!/2!(n-1)!](-e^2)\\&\quad\times\int A_\mu(x^i)A_\nu(x^k)(-\phi^*(x^i)\phi(x^k)\\&\quad\times\langle P(\partial_\mu{}^{(i)}\phi(x^i),\,\partial_\nu{}^{(k)}\phi^*(x^k))\rangle_0\\&\quad-\phi(x^i)\phi^*(x^k)\langle P(\partial_\mu{}^{(i)}\phi^*(x^i),\,\partial_\nu{}^{(k)}\phi(x^k))\rangle_0 d_4x^k\\&=[(-i)^n/n!]\cdot in/2\cdot e^2\int A_\mu(x^i)A_\nu(x^k)in_\mu n_\nu\\&\qquad\times(\phi^*(x^i)\phi(x^k)+\phi(x^i)\phi^*(x^k))\delta(x^i-x^k)d_4x^k\\&=-[(-i)^n/n!]ne^2\phi^*(x^i)\phi(x^i)(n_\mu A_\mu(x^i))^2.\qquad(22')\end{aligned}$$

This term, therefore, exactly cancels the term (21). It follows that for the case $A_\mu{}^e=0$ all normal-dependent terms cancel identically.[10]

The S matrix for $A_\mu{}^e\neq0$ can be obtained from the S matrix for $A_\mu{}^e=0$ by the replacement $A_\mu\to A_\mu+A_\mu{}^e$. However, the above argument [following Eq. (15′)] is independent of such a replacement. The identical cancellation of all normal-dependent terms is therefore generally valid. In the following we shall drop these terms in the scattering matrix.

One can write the Hamiltonian

$$\begin{aligned}\mathcal{H}^i[x]=&ie\phi^*(x)(A_\mu+A_\mu{}^e)(\partial_\mu-\partial_\mu{}^*)\phi(x)\\&+e^2\phi^*(x)(A_\mu+A_\mu{}^e)(A_\mu+A_\mu{}^e)\phi(x).\end{aligned}$$

∂_μ and $\partial_\mu{}^*$ are defined to act only on $\phi(x)$ and $\phi^*(x)$, respectively. All P brackets of pairs $\phi(x^i)\phi^*(x^k)$ will be given by (13) and the differentiations are properly taken into account by inserting for each linear factor $A_\mu(x)+A_\mu{}^e(x)$ a factor $\partial_\mu-\partial_\mu{}^*$ between the pair of P brackets containing x, e.g., $\Delta_F(x'-x)(\partial_\mu-\partial_\mu{}^*)\Delta_F(x-x'')$. ∂_μ and $\partial_\mu{}^*$ will therefore act, respectively, on the first and the second variable in the argument of Δ_F.

For the general case $A_\mu{}^e\neq0$ we may look for the radiative corrections of order n' for a system of m mesons and p photons interacting with each other and with an external field to order f' in this field. The terms of (11) contributing in this case will be given by

$$n_{\max}=p+f'+n'\geqslant n\geqslant\begin{cases}(p+f'+n')/2, & p+f'\text{ even}\\(p+f'+n'+1)/2, & p+f'\text{ odd}\end{cases}\qquad(23)$$

where n and n' are defined as before. The term with the largest contributing n will involve only those parts of $\mathcal{H}[x]$ which are linear in A_μ and/or only those parts of $\mathcal{H}^e[x]$ which are linear in $A_\mu{}^e$. It will not involve $\mathcal{H}^c[x]$. We now associate a definite set of integration variables with the operators referring to the real particles and external fields, and determine a definite division of the remaining operators into P brackets of pairs as described before. It is easily seen that for each such choice the integral can be brought into a one-to-one correspondence with a Feynman diagram, in complete analogy with the electron case as given in **I**. Each of the $n_{\max}=p+f'+n'$ variables x^k will be represented by a world point in a space-time diagram. Each operator $A_\mu(x^i)$ annihilating an incoming (creating an outgoing) real photon will be represented by a photon world line drawn from the point x^i to $-\infty\,(+\infty)$ with an arrow in its positive time direction of propagation. Each external field $A_\mu{}^e(x^j)$ will be represented by a cross at the point x^j. Each operator $\phi(x^i)$ annhihilating a positive meson (or creating a negative meson), and each operator $\phi^*(x^i)$ creating a positive meson (or annihilating a negative meson) will be represented by a meson world line from x^i to $-\infty$ (or $+\infty$) and $+\infty$ (or $-\infty$), respectively, with arrows in the positive (or negative) time direction of propagation. The world lines of real mesons and photons will be called "external lines." Each function $D_F(x^i-x^k)$ resulting from the vacuum expectation value of the P bracket of a pair $A_\mu(x^i)A_\nu(x^k)$ according to (12) will be represented by an "internal photon line" from the point x^i to the point x^k without an arrow. Each function $\Delta_F(x^i-x^k)$ resulting from the vacuum expectation value of a P bracket of a pair

[10] A similar proof for a different case was sketched by P. T. Matthews, Phys. Rev. 76, 684 (1949).

$\phi^*(x^i)\phi(x^k)$ according to (13), (14), or (15′) will be represented by an "internal meson line" from x^i to x^k with an arrow pointing from x^i to x^k. The resulting diagram will contain meson lines which, following the arrows, will lead from $-\infty$ (or $+\infty$) through the diagram to $+\infty$ (or $-\infty$) for positive (or negative) mesons without ever meeting each other. It will also contain, in general, lines which are composed of internal meson lines only, and which form "closed loops" with all arrows pointing in the same sense. The meson lines will be interconnected by internal photon lines such that each point of the diagram has exactly one (internal or external) meson line incident and one (internal or external) meson line outgoing in the sense of the arrows. It will also be either one end of an internal or external photon line or it will contain a cross indicating the action of the external field.

A typical integral may lead to a diagram where all lines are interconnected, or to one which consists of two or more unconnected parts. Assume that such a part is not associated with external meson or photon lines, or with the external field. In this case it will correspond to a part of the integrand which can be integrated independently of the rest, yielding a constant numerical factor. When all radiative corrections were taken into account one would find that each diagram is associated with all possible unconnected diagrams of this kind. These unconnected diagrams and their corresponding integrals evidently occur when one calculates the S matrix for a vacuum remaining a vacuum when no mesons, photons, or external fields are present. Since this process has unit probability these numerical factors will add up to a phase factor which we may choose to be unity. It follows that all disconnected diagrams without external lines or crosses can be disregarded and their corresponding integrals put equal to zero.

We have seen above that for $n=n_{\max}$ each point or "corner" of a diagram has exactly three lines—two meson lines and one photon line—connecting it with the remainder of the diagram. (The photon line may be replaced by a cross indicating the action of A_μ^e.) In the quantum electrodynamics of the electron these are the only diagrams possible. We shall call them "single-corner diagrams," because there is only a single A_μ or A_μ^e associated with each corner.

For $n<n_{\max}$ the integrals will not correspond to single-corner diagrams. Consider the case $n=n_{\max}-1$. The diagram corresponding to this integral will again have n corners, since n is the number of integration variables (in terms of four-vectors). It will therefore have one corner less than the diagram discussed previously. The integral will also differ from the previous one in that two factors containing a single operator $A_\mu(x^k)$ or $A_\mu^e(x^k)$ each will be replaced by one factor containing $A_\mu(x^k)A_\mu(x^k)$, $A_\mu^e(x^k)A_\mu^e(x^k)$ or $A_\mu(x^k)A_\mu^e(x^k)$. These factors arise from the terms of $\mathcal{H}$ and $\mathcal{H}^e$ quadratic in the electromagnetic field, or from $\mathcal{H}^c$. The point

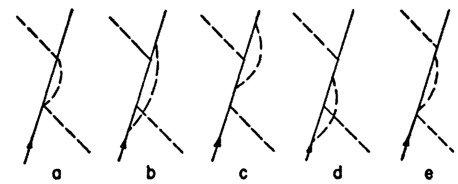

FIG. 2. Diagram a can be obtained by shrinkage of internal meson lines from any one of the diagrams b, c, d, and e. It has therefore weight 4.

x^k will therefore be associated with *two* electromagnetic field operators. We will refer to such a point as a "double corner." A double corner at x^k can arise from any of the following combinations:

$$A_\mu(x^k)A_\mu(x^k),\quad A_\mu(x^k)A_\mu^e(x^k),\quad A_\mu^e(x^k)A_\mu^e(x^k), \tag{24a}$$

$$\begin{gathered} A_\mu(x^k)\langle P(A_\mu(x^k)A_\nu(x^i))\rangle_0, \\ A_\mu^e(x^k)\langle P(A_\mu(x^k)A_\nu(x^i))\rangle_0, \end{gathered} \tag{24b}$$

$$\begin{gathered} \langle P(A_\lambda(x^e)A_\mu(x^k))\rangle_0\langle P(A_\mu(x^k)A_\nu(x^i))\rangle_0, \\ \langle P(A_\mu(x^k)A_\mu(x^k))\rangle_0. \end{gathered} \tag{24c}$$

The first line refers to "external double corners" with two external photon lines, one external photon line and one cross, or two crosses at the point x^k, respectively (see Fig. 1). The second line gives "mixed double corners." These are corners with one internal photon line and either one external photon line or one cross. Finally, there can be "internal double corners" where two internal photon lines meet, or where the two ends of one internal photon line meet, as sometimes happens. The diagram with $n=n_{\max}-1$ will also lack one pair $\phi\phi^*$ as compared to the one with $n=n_{\max}$. Since the same number of real mesons are involved this means that there will be one $\langle P(\phi(x^k)\alpha^*(x^e))\rangle_\lambda$ less, corresponding to one missing internal meson line. Let x^i and x^k be two adjacent corners connected by one internal meson line in a single-corner diagram from $n=n_{\max}$. There will be one of the diagrams arising from $n=n_{\max}-1$ which differs from this one only with respect to the corners x^i and x^k; i.e., it will have one double corner x^i, say, instead of the two single corners. The photon lines (or crosses) associated with x^i and x^k will now meet at this double corner. Therefore to every diagram with a double corner there corresponds a single-corner diagram from which it can be obtained by "shrinkage" of one internal meson line to zero. It is clear that the next smaller value of n will lead to diagrams with two double corners which can again be obtained from diagrams with one double corner by shrinkage of one internal meson line, or from single-corner diagrams of shrinkage of two meson lines. This process can be continued until all (or all but one) corner of the single-corner diagrams have been shrunk into double corners, corresponding to the integral with $n=n_{\max}/2$ [or $(n_{\max}+1)/2$] as seen from (23). Since there occur in $\mathcal{H}^i$ never more than two operators A_μ and/or A_μ^e with the same argument, no diagram can have a triple (or higher) corner, and, therefore, a meson line can be shrunk only when it connects two single corners.

It is an immediate consequence of the structure of the integrals (11) that, on shrinking all single-corner diagrams in all possible ways one obtains all diagrams with one or more double corners ("double-corner diagrams") which correspond to the integrals with $n<n_{\max}$. However, it can occur that shrinkage of two different single-corner diagrams may lead to the same double-corner diagram. The number of times a particular double-corner diagram arises from shrinkage will be called its "weight." As an example the diagram a of Fig. 2 can be obtained by shrinkage from each of the single-corner diagrams b, c, d, or e. It has therefore weight 4.

We shall first calculate the weight directly from the integrals. One observes that

$$\begin{aligned}&\langle P(A_\lambda(x^e)A_\mu(x^k)A_\mu(x^k)A_\nu(x^i))\rangle_0\\&=\delta_{\mu\sigma}\langle P(A_\lambda(x^e)A_\mu(x^k)A_\sigma(x^k)A_\nu(x^i))\rangle_0\\&=2\langle P(A_\lambda(x^e)A_\mu(x^k))\rangle_0\langle P(A_\mu(x^k)A_\nu(x^i))\rangle_0\\&\qquad+\langle P(A_\lambda(x^e)A_\nu(x^i))\rangle_0\langle P(A_\mu(x^k)A_\mu(x^k))\rangle_0.\end{aligned}$$

Each internal double corner [first term of (24c)] will therefore contribute a factor 2 to the weight of the diagram, except when it stems from a single internal photon line [second term of (24c) and Fig. 3a]. However,

$$\begin{aligned}&\langle P(A_\mu(x^k)A_\mu(x^k)A_\nu(x^i)A_\nu(x^i))\rangle_0\\&\qquad=2\langle P(A_\mu(x^k)A_\nu(x^i))\rangle_0\langle P(A_\mu(x^k)A_\nu(x^i)\rangle_0\\&\qquad\qquad+\langle P(A_\mu(x^k)A_\mu(x^k))\rangle_0\langle P(A_\nu(x^i)A_\nu(x^i))\rangle_0,\end{aligned}$$

such that, when two internal double corners are connected to each other by two photon lines, their combined contribution to the weight of the diagram will be 2 rather than 4 (Fig. 3b). Each mixed double corner also contributes a factor 2: the second combination (24b), because of the factor 2 in $\mathcal{H}^e$ of Eq. (10), and the first one, because each $A_\mu(x^k)$ may occur inside the P bracket.

$$\begin{aligned}&\delta_{\mu\sigma}\langle P(A_\mu(x^k)A_\sigma(x^k)A_\nu(x^i))\rangle_1\\&\quad=\delta_{\mu\sigma}A_\mu(x^k)\langle P(A_\sigma(x^k)A_\nu(x^i))\rangle_0\\&\qquad\qquad+\delta_{\mu\sigma}A_\sigma(x^k)\langle P(A_\mu(x^k)A_\nu(x^i))\rangle_0\\&\quad=2A_\mu(x^k)\langle P(A_\mu(x^k)A_\nu(x^i))\rangle_0.\end{aligned}$$

There will also be a factor 2 from $\mathcal{H}^e$ in the external double corner arising from $A_\mu A_\mu{}^e$ in (24a). In the first term of (24a) each of the operators $A_\mu(x^k)$ may be associated with either of the two real photons emitted or absorbed. One is thus lead to two integrals which eventually are identical. It is convenient, therefore to write only one integral for each factor $A_\mu A_\mu$ and to give

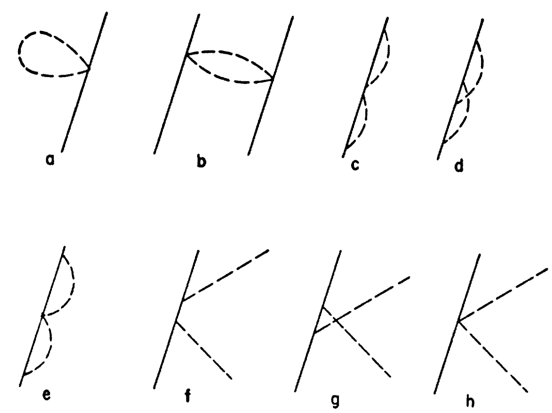

FIG. 3. Examples for the discussion of the weight factor.

it weight 2, thereby permitting only one choice of association.

We summarize these considerations in the simple weight formula

$$w=2^g,\quad g=d-d_f-a-b, \tag{25}$$

where d is the number of double corners, d_f is the number of double corners with two crosses, a is the number of closed photon lines (Fig. 3a), and b is the number of pairs of double corners connected by two photon lines (Fig. 3b).

It remains to show that w of (25) is exactly the number of different single-corner diagrams which by shrinkage give the same double-corner diagram. Clearly, when two (internal or external) photon lines end at neighboring single corners, they can come in "parallel" or "crossed," as is shown for the corners 1 and 2 of Figs. 3c, d and Figs. 3f, g. The two corresponding single-corner diagrams will both shrink to the same double-corner diagram (Figs. 3e, h). Furthermore, an external photon line (or cross) can be incident on either side of an internal single corner. The two diagrams will again shrink to the same mixed double corner. On the other hand, there is obviously only one way to obtain a double corner with 2 crosses or with a closed photon line. Finally, it is seen that the double-connected double corners of Fig. 3b can be obtained in only 2 ways rather than 4 ways, i.e., from either of the two diagrams Figs. 12a and b.

The above analysis shows that all single-corner diagrams from the integral $n=n_{\max}$ together with all different double-corner diagrams obtained from them by shrinkage and weighted according to Eq. (25) give exactly all diagrams resulting from the S matrix (11) for n satisfying (23).

We can now formulate a recipe for the calculation of the S matrix (11). Gives m mesons and p photons in interaction with each other and with an external field, we can find the radiative corrections of order n' which are of order f' in the external field, by the following procedure:

(1) Draw all possible connected single-corner dia-

grams with $n=n_{\max}=n'+p+f'$ corners, m external meson lines, p external photon lines, and f' external field interactions.

(2) Find all possible double-corner diagrams by shrinkage of the single-corner diagrams.

(3) Write down an integral for each diagram as follows:

(a) Label the corners with x^1, x^2, $\cdots x^n$ and associate with each single corner one, with each double corner two polarizations μ, ν, $\cdots$.

(b) At each corner x^k with polarization μ insert $A_\mu^e(x^k)$ for a cross, $A_\mu(x^k)$ for an external line, and $\phi(x^k)$ or $\phi^*(x^k)$ for an external meson line according to its arrow direction in or out of the diagram.

(c) For each two corners x^i and x^k insert for each connecting photon line a factor $\frac{1}{2}\delta_{\mu\nu}D_F(x^i-x^k)$, and for each connecting mesons line a factor $\frac{1}{2}\Delta_F(x^i-x^k)$, if the arrow points from x^k to x^i.

(d) For each single corner x^k with polarization μ insert $ie(\boldsymbol{\partial}_\mu{}^{(k)}-\boldsymbol{\partial}_\mu{}^{*(k)})$ where $\boldsymbol{\partial}_\mu{}^{*(k)}$ differentiates one term of the form $\Delta_F(x^i-x^k)$ or $\phi^*(x^k)$ and $\boldsymbol{\partial}_\mu{}^{(k)}$ differentiates one term of the form $\Delta_F(x^k-x^i)$ or $\phi(x^k)$.

(e) For each double corner x^k with polarizations μ and ν insert $e^2\delta_{\mu\nu}$.

(f) Integrate over all x^k $(k=1, 2, \cdots n)$ and multiply by $(-i)^n w$, where w is given for each diagram by (25). (Note that the factor $1/n!$ occurring for each such diagram is canceled, since there are $n!$ ways of labeling the same diagram with x^1, $\cdots x^n$ which all give the same integral.)

(4) Sum these integrals and find that part of the S matrix (11) which satisfies (23) for the problem under consideration.

For actual calculations it will be convenient to work in momentum space. The Fourier transforms are[11]

$$A_\mu(x)=(2\pi)^{-2}\int A_\mu(k)\delta(k^2)\exp(ik_\lambda x_\lambda)d_4k, \tag{26a}$$

$$A_\mu^e(x)=(2\pi)^{-2}\int A_\mu^e(k)\exp(ik_\lambda x_\lambda)d_4k, \tag{26b}$$

$$\phi(x)=(2\pi)^{-2}\int \phi(p)\delta(p^2+m^2)\exp(ip_\lambda x_\lambda)d_4p, \tag{27a}$$

$$\phi^*(x)=(2\pi)^{-2}\int \phi^2(p)\delta(p^2+m^2)\exp(-ip_\lambda x_\lambda)d_4p, \tag{27b}$$

$$\begin{aligned}D_F(x)&=(2\pi)^{-2}\int \frac{1}{\pi}\delta_+(k^2)\exp(ik_\lambda x_\lambda)d_4k\\ &=-2i(2\pi)^{-4}\int\left(\frac{1}{k^2}+i\pi\delta(k^2)\right)\exp(ik_\lambda x_\lambda)d_4k,\end{aligned} \tag{28a}$$

$$\begin{aligned}\Delta_F(x)&=(2\pi)^{-2}\int \frac{1}{\pi}\delta_+(p^2+m^2)\exp(ip_\lambda x_\lambda)d_4p\\ &=-2i(2\pi)^{-4}\int\left(\frac{1}{(p^2+m^2)}+i\pi\delta(p^2+m^2)\right)\\ &\qquad\times\exp(ip_\lambda x_\lambda)d_4p.\end{aligned} \tag{28b}$$

The functions $\delta_\pm(x)$ are defined by

$$\delta_\pm(x)=\left(\frac{1}{2\pi}\right)\int_0^\infty \exp(\pm i\alpha x)d\alpha=\tfrac{1}{2}\delta(x)\pm\frac{1}{(2\pi ix)}. \tag{29}$$

When the transformation to momentum space is carried out in this way, and when all the integrations over x^1, $\cdots x^n$ are performed, the resultant S matrix will be very similar in form to the S matrix in coordinate space. In fact, it can be obtained from the latter by simple replacements, such that we can restate the construction recipe (3) for momentum space:

(3′) Write down an integral in momentum space for each diagram as follows:

(a′) Label all meson lines with four-momenta p, p', p'', $\cdots$, all photon lines with momenta k, k', k'', $\cdots$, and all crosses with q, q', q''. Associate with each single corner one, with each double corner two polarizations μ, ν, $\cdots$.

(b′) Insert $A_\mu^e(q)$ for a cross, $A_\mu(k)$ for an external photon line, and $\phi(p)\delta(p^2+m^2)$ or $\phi^*(p)\delta(p^2+m^2)$ for an external meson line pointing into or our of the diagram, respectively.

(c′) Insert for each internal photon line a factor $\delta_{\mu\nu}$ times the photon propagation function[11] $1/k^2$; insert for each internal meson line the meson propagation function $1/(p^2+m^2)$.

(d′) Insert for each single corner with polarization μ a factor[12] $(p_\mu+p_\mu')\delta(p-p'\pm k)$, where p_μ and p_μ' are the momenta associated with the meson lines leading into and out of the corner, and k is the momentum associated with the internal or external photon line ending there. If there is a cross instead of an external photon line k is to be replaced by q.

(e′) For each double corner insert a factor $-\delta_{\mu\nu}\delta(p-p'\pm k\pm k')$. One or both of the photon momenta k, k' may be replaced by external field momenta q, q'.

(f′) Integrate over all momenta and multiply each integral by its respective weight w as given in Eq. (25). Multiply each integral by the same factor

$$(-i)^{(n_{\max}-E)/2}(e/4\pi^2)^{n_{\max}}. \tag{30}$$

This factor depends only on the number of participating particles and on the order of approximation. E is the total number of external lines and crosses,

$$E=2m+p+f'. \tag{31}$$

[11] When the integrations in the S matrix are carried out in the manner explained in **II**, the δ-functions in Eqs. (28a) and (28b) can be dropped.

[12] It is clear that, if at one end of an internal photon line the δ-function is (arbitrarily) written with $+k$, the δ-function at the other end of the same internal photon line must be written with $-k$.

These rules follow from the rules (3) given above in the following way. Let F_m and F_p be the number of internal photon lines and meson lines for a given diagram. The structure of the diagrams tells us that

$$2F_p=n', \quad F_m=n-m \tag{32}$$

and that the total number of internal lines

$$F=F_m+F_p=n+\tfrac{1}{2}(n_{\max}-E)=\tfrac{1}{2}(3n_{\max}-E)-d \tag{33}$$

where $d=n_{\max}-n$ is the total number of double corners. The integral in coordinate space for a particular diagram will be multiplied by its weight w and by $(-i)^n$ as explained in rule (3f). The Fourier transforms (26) to (29) yield an additional factor $(2\pi)^{-2E}$ and rule (3′b′) for the external lines and crosses, a factor $(-i)^F(2\pi)^{-4F}$ and rule (3′c′) for the internal lines, a factor $(-e)^s(2\pi)^{4s}$ and rule (3′d′) for the single corners (s is the number of single corners), and a factor $(-e^2)^d(2\pi)^{4d}$ and rule (3′e′) for the double corners. The factors $(2\pi)^{4s}$ and $(2\pi)^{4d}$ came from the x-integrations which each yield $(2\pi)^4$ and a δ-function. Thus the total factor is

$$\begin{aligned}(-i)^{-m+n'/2}(e/4\pi^2)^{n_{\max}}\\ =i^{m-n'/2}(\alpha/\pi)^{n'/2}(e/4\pi^2)^{p+f'}(1/2\pi)^{n'},\end{aligned} \tag{30'}$$

which is the same as (30). In (30′) we inserted the fine-structure constant $\alpha=e^2/4\pi\cong 1/137$. It should be noted that the factor (30′) is also valid for the electron case where double-corner diagrams do not exist, and where $n=n_{\max}$ always. Equation (30′) shows that the natural expansion parameter in perturbation theory is[13] α/π.

The rules (1), (2), (3′), and (4) are those of the Feynman theory[14] for the construction of the scattering matrix. We have thus shown that Feynman's S matrix is identical with the S matrix (11) of the Schwinger-Tomonaga theory.

III. ENUMERATION OF POSSIBLE PRIMITIVE DIVERGENCIES

A primitive divergent diagram is defined (as in I) as a diagram whose integral diverges such that when any of the internal lines is cut and thus replaced by two external lines, the resulting integral is convergent.

It is easy to enumerate the possibly primitive divergent processes for the interaction of any type of "source particles" (charged particles of spin 0, $\frac{1}{2}$, 1, nucleons) with any type of corresponding "interaction particles" (photons, mesons) and external fields. For all these cases it is sufficient to restrict oneself to single-corner diagrams, as will be proven in the next section for charged spinless mesons interacting with photons and an external field. Each single corner of these diagrams will either have one external field acting or none. In the first case there will be a cross at that corner and but two "source lines" or two "interaction lines" leading to it. In the second case there will always be exactly two source lines and one interaction line. A typical diagram will have n corners, E_i external lines corresponding to E_i ingoing and/or outgoing interaction particles, and E_s external source lines corresponding to $E_s/2$ participating source particles. There may also be external fields interacting f_s times with the source particles and f_i times with the interaction particles. The resulting diagrams will therefore have

$$F_i=\tfrac{1}{2}(n-E_i-f_s+f_i) \tag{34a}$$

internal interaction lines and

$$F_s=n-f_i-E_s/2 \tag{34b}$$

internal source lines, yielding

$$F=\tfrac{1}{2}(3n-f_i-f_s-E_i-E_s)=\tfrac{1}{2}(3n-E) \tag{34c}$$

internal lines. $E=E_s+E_i+f_s+f_i$ is the total number of external lines and crosses.

Quite generally, an internal line will correspond to a propagation function which is a polynomial divided by a quadratic in the momentum associated with it. The propagation functions

$$1/k^2, \quad 1/(p^2+m^2), \quad (ip_\mu\gamma_\mu-m)/(p^2+m^2) \tag{35}$$

are examples for a photon, a spinless meson, and a Dirac particle (electron or nucleon), respectively. We shall denote the degree of the polynomial in the numerator of the propagation function of source and interaction particles by D_s and D_i. Each corner will contain a δ-function of the three associated momenta and a polynomial of degree D_c.

$$(p_\mu+p_\mu')\delta(p-p'+k), \quad \gamma_\mu\delta(p-p'+k)$$

are examples for the interaction of spinless mesons with photons, and of nucleons (or electrons) with mesons of spin 1 (or photons).

Consider a single-corner diagram which is at most primitive divergent when integrated over the F internal momentum four-vectors. The n δ-functions of the corners permit to eliminate $n-1$ of them, since the last δ-function will contain the external momenta only, expressing energy-momentum conservation. The integral will be convergent if the degree of the denominator exceeds the degree of the numerator (including the differentials d_4p, d_4p', $d_4k\cdots$) by at least one. Since the degree of the denominator is $2F$, as seen from (35), the convergence condition is

$$D_{\text{den}}-D_{\text{num}}-4(F-n+1)\geqslant 1$$

or

$$4n-2F-D_{\text{num}}=n+E-D_{\text{num}}\geqslant 5 \tag{36}$$

by (34c).

With the above definitions

$$\begin{aligned}D_{\text{num}}&=D_sF_s+D_iF_i+D_cn\\&=D_s(n-f_i-E_s/2)+\tfrac{1}{2}D_i(n-E_i-f_s+f_i)+D_cn.\end{aligned}$$

[13] As will be shown in the next section, the number of non-trivial integrations is $F+1-n_{\max}=1-m+n'/2$. Each of these contribute a factor $i\pi^2$, such that there remains only one factor i and the factor $\pi^{-n'}$ is replaced by π^{1-m}.

[14] They are given for spinless mesons in Feynman's second paper, reference 5. Note, however, that Feynman uses Gaussian units and a different definition of the metric tensor.

Equation (36) becomes

$$n(1-D_s-D_c-Di/2)+E+D_s(f_i+E_s/2) \\ +\tfrac{1}{2}D_i(E-E_s-2f_i)\geqslant 5. \quad (37)$$

This inequality is a sufficient convergence condition for a diagram which is not worse than primitively divergent.[15] The condition is not necessary, because the highest powers of the internal momenta may cancel identically in the integrand.[16] Further cancellation may occur between different diagrams for the same process, such that a process may be completely finite, although (37) is not fulfilled for each individual diagram. Such cancellation indeed occurs in the scattering of light by light and associate phenomena (see items 4a and 4b below) via particles of spin 0, $\frac{1}{2}$, and 1, but it requires the inclusion of possible double-corner diagrams.

If a process involving $E_s/2$ source particles and E_i interaction particles is to yield convergent results in arbitrary high order, (37) requires that the coefficient of n be positive. Therefore,

$$D_s+D_c+D_i/2\leqslant 1 \quad (38)$$

must be satisfied for the elimination of primitive divergencies.

All meson theories of nuclear forces have $D_s=1$ [see (35)] and therefore (38) would require $D_c=D_i=0$. This implies mesons of spin 0 and no derivative coupling;[17] i.e., scalar (or pseudoscalar) theory with scalar (or pseudoscalar) coupling. For those two cases the convergence condition (37) yields

$$E+\tfrac{1}{2}E_s+f_i=\tfrac{3}{2}E_s+E_i+2f_i+f_s\geqslant 5. \quad (39)$$

This condition is the same for the electrodynamics of the electron (see **I**) and the same *possible* primitive divergencies arise. However, the scattering of mesons by mesons (via nucleons) does not converge as does the corresponding scattering of light by light in electrodynamics. As mentioned previously, the latter is formally due to fortuitous cancellation, but has a deeper reason in the condition of gauge invariance. The divergence of meson-meson scattering cannot be removed by mass or charge renormalization. An infinite direct interaction must be introduced into the Hamiltonian which cancels the divergence.[18] This procedure together with mass and charge renormalization removes all the infinities from the S matrix.

In quantum electrodynamics we have $D_i=0$, and (38) permits either $D_s=1$ and $D_c=0$ or $D_s=0$ and $D_c=1$. The former values arise for the electron (see **I**), the latter for the spinless meson. Since f_i cannot occur here, the convergence condition (37) is

$$E_s+E_i+f_s=E\geqslant 5. \quad (40)$$

This condition, however, need only be applied to diagrams with $n\geqslant E$ for the following reason. Clearly, the integral will converge if the $n-1$ available δ-functions eliminate all internal momenta, i.e., if $F=n-1$. From (34c) we see that this means $n=E-2$, and that $n-E$ is always an even number. Therefore only diagrams with $n\geqslant E$ can diverge.

The possible primitive divergencies are therefore the following:[19]

(1) The meson self-energy[20] ($E_s=2$, $E_i=f_s=0$, quadratic divergence).

(2a) The photon self-energy ($E_i=2$, $E_s=f_s=0$, quadratic divergence).

(2b) The polarization of the vacuum ($f_s=2$, $E_s=E_i=0$, quadratic divergence).

(3) The "Lamb shift" and radiative corrections to the scattering of a meson in an external field to first order in this field ($E_s=2$, $F_s=1$, $E_i=0$, linear divergence).

(4a) The scattering of light by light ($E_i=4$, $E_s=f_s=0$, logarithmic divergence).

(4b) The scattering of light by an external field to second order in this field ($E_i=2$, $F_s=2$, $E_s=0$, logarithmic divergence).

(5a) The radiative corrections of the "Compton effect" ($E_s=2$, $E_i=2$, $f_s=0$, logarithmic divergence).

(5b) The radiative corrections to "bremsstrahlung," i.e., emission or absorption of a photon by a meson in an external field to first order in that field ($E_s=2$, $E_i=1$, $f_s=1$, logarithmic divergence).

(5c) The "Lamb shift" and radiative corrections to meson scattering to second order in the external field ($E_s=2$, $F_s=2$, $E_i=0$, logarithmic divergence).

(6) The radiative corrections to meson-meson scattering[20] ($E_s=4$, $E_i=f_s=0$, logarithmic divergence).

There is actually one more possible divergent process, i.e., the scattering of light by an external field to first order in that field ($E_i=2$, $f_s=1$, $E_s=0$, linear divergence). However, this process involves a closed loop with an odd number of corners and therefore vanishes identically by Furry's theorem. This theorem is obviously valid here as in the electron case, because ϕ and the charge conjugate solution ϕ^* fulfill the same equation except for a change in the sign of the charge e. Since two internal meson lines with opposite arrows correspond to vacuum expectation values of operators which are charge conjugate to each other, two closed loops with n corners each and opposite arrow directions will differ only in the respective factors e^n and $(-e)^n$. If n is odd two diagrams which differ only in the arrow

[15] The use of Kemmer-Duffin matrices for spin 0 and 1 leads to a sufficient condition which is more restrictive (see reference 7).

[16] Such cancellation seems very fortuitous and indeed occurs only if the combination of propagation function and coupling exhibit a certain "redundancy" as in the case of vector mesons interacting with photons.

[17] The propagation functions and couplings for various meson theories are given in Feynman's second paper, reference 5.

[18] Very recently this program was carried through to all order in the coupling constant by P. T. Matthews (see reference 3).

[19] This result and the conclusions of Section V of this paper were first presented by the author at the New York meeting of the American Physical Society January 1950. See Phys. Rev. **78**, 346 (1950).

[20] Note that according to our definition of n', the lowest order to which the process occurs is the second-order radiative correction, $n'=2$.

direction of their closed loop of n corners will cancel identically. This result is unchanged by shrinkage of any of the meson lines in the closed loop.

In the next section we shall show how the infinities can be separated and removed from the S matrix by renormalizations, such that the resultant, renormalized S matrix leads to finite values for all the processes (1) to (6).

IV. REMOVAL OF THE DIVERGENCIES BY RENORMALIZATION

A. General Considerations

The divergence properties of single-corner diagrams derived in the last section can easily be generalized to double-corner diagrams. According to rule (3′) of Section II the shrinkage of two neighboring single corners involves the replacement of a factor

$$\delta(p-p''+k)(p_\mu+p_\mu'')(p''^2+m^2)^{-1}(p_\nu''+p_\nu')\times\delta(p''-p'+k')$$

by

$$-\delta_{\mu\nu}\delta(p-p'+k+k')$$

and also requires a corresponding change in the weight factor. We have, therefore, one δ-function less, but also one less integration over internal momenta, such that the number of independent variables remains unchanged. Since the difference $D_{\text{den}}-D_{\text{num}}=0$ in both factors, the resultant double-corner diagram will diverge (or converge) exactly as the original diagram. It follows that every primitive divergent single-corner diagram yields by shrinkage a double-corner diagram of the same order of divergence. The list of primitive divergents (1) to (6) is therefore also valid for the corresponding double-corner diagrams.

An unambiguous separation of a primitive divergent integral into an infinite and a finite part can be accomplished as for the electron (see **II**) by a Maclaurin expansion of the integrand in terms of the external momenta p_μ

$$R(p,t)=R(0,t)+p_\mu(\partial/\partial p_\mu)R(0,t)+\tfrac{1}{2}p_\mu p_\nu(\partial^2/\partial p_\mu\partial p_\nu)R(0,t)+\cdots. \quad (41)$$

$R(p,t)$ is the integrand after the integrations over the δ-function are carried out and the operators ϕ^*, ϕ, A_μ, and $A_\mu{}^e$ are omitted. p_μ and t_μ are typical external and internal momenta, respectively. Since each differentiation increases $D_{\text{den}}-D_{\text{num}}$ by unity, a logarithmically, linearly, or quadratically divergent integral will have an expansion of R in which only the first one, two, or three terms give divergencies. The form of the divergent terms follows from relativistic invariance.

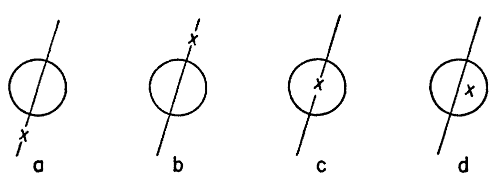

FIG. 4. The meson scattering diagrams to first order in the external field.

For example, the first term of (41) for the scattering of light by light, and of light by an external field yields a logarithmically divergent integral whose integrand is

$$A_\mu(p^1)A_\nu(p^2)A_\lambda(p^3)A_\sigma(p^4)T_{\mu\nu\lambda\sigma}\delta(p^1+p^2+p^3+p^4)$$

and

$$A_\mu(p^1)A_\nu(p^2)A_\lambda(p^3)A_\sigma(p^4)U_{\mu\nu\lambda\sigma}\delta(p^1+p^2+p^3+p^4), \quad (42)$$

respectively, after the integrations over the internal momenta $l^{(i)}$ are carried out. The tensors $T_{\mu\nu\lambda\sigma}$ and $U_{\mu\nu\lambda\sigma}$ are independent of the p^k, such that the terms (42) are gauge-variant. Since the theory is gauge-invariant the sum of the terms (42) over all diagrams of any given order n' must vanish;[21] i.e., $\Sigma T_{\mu\nu\lambda\sigma}=0$ and $\Sigma U_{\mu\nu\lambda\sigma}=0$. This will be verified to lowest order ($n'=0$) in the next section. We are therefore permitted to regard the processes of type (4) in the list of primitive divergencies as completely finite.

These arguments may not seem to be satisfactory, since $T_{\mu\nu\lambda\sigma}$ and $U_{\mu\nu\lambda\sigma}$ are divergent integrals. In view of these and similar arguments further on, we assume, therefore, that all integrations are carried out with regulators. This implies the introduction in the Lagrangian of auxiliary fields with suitably chosen masses and coupling constants.[22] The conditions on the auxiliary masses and coupling constants are such that all integrals which diverge worse than logarithmic are put equal to zero. Logarithmically divergent integrals become finite, but regulator-dependent. The masses are assumed to become infinite after the integration is completed, such that originally convergent integrals remain unaltered and independent of the regulators.[23] The use of regulators makes the arguments concerning divergencies, like the one following (42), mathematically meaningful.[24]

[21] A formal proof can be given in complete analogy with the one for the electron case given by J. C. Ward, Phys. Rev. **77**, 293 (1950), since the relation (A4) (see Appendix I) which is needed in this proof is obviously valid.

[22] The introduction of the auxiliary fields in the Lagrangian rather than in the S matrix is required, because they change the equations of motion and the momentum energy tensor, as is seen in the calculation of the self-stress. For the problems considered in this paper, however, it is irrelevant where the regulators are introduced. See F. Rohrlich, Phys. Rev. **77**, 357 (1950).

[23] The notion of logarithmic divergence and cut-off dependence are in this sense equivalent. Also, in the following, "finite" and "convergent" will mean "finite and cut-off independent" unless otherwise stated.

[24] Note that the use of regulators does not imply a loss of generality, since all one can study meaningfully is how the S matrix would behave if the theory were finite (which here also requires the assumption of the—unproven—existence of the expansion in the fine-structure constant). The finiteness of the theory achieved in this way guarantees gauge-invariance. The charge-renormalization procedure is not a requirement of gauge-invariance. Mass, charge, and direct interaction renormalization are required only in order to avoid imposing conditions on the regulators in addition to those which guarantee finiteness (e.g., $\Sigma c_i \ln m_i=0$ instead of the weaker condition $\Sigma c_i \ln m_i=$finite). Whether or not such conditions are introduced is irrelevant for

We now return to Eq. (41) for the purpose of general arguments. Again, on the basis of relativistic invariance the first, linearly divergent term of a primitive divergent meson scattering diagram (item 3 on the list of divergencies) is seen to vanish identically, such that these diagrams actually diverge only logarithmically. The second term of (41) gives therefore the only infinite term which is of the form

$$\phi^*(p^1)\phi(p^2)(p_\mu{}^1+p_\mu{}^2)A_\mu{}^e(p^1-p^2) \tag{43}$$

after the integration over the internal momenta t has been performed. A similar term containing $(p_\mu{}^1-p_\mu{}^2)\times A_\mu{}^e(p^1-p^2)$ must vanish identically, since it is not gauge-invariant.

Similarly, the only divergent term of a primitive divergent diagram of type (5) (Compton effect and related phenomena) will be of the form

$$\phi^*(p^1)\phi(p^2)A_\mu(k)A_\mu(p^1-p^2+k). \tag{44}$$

Consider now the radiative corrections of order n' to the scattering of a meson by an external field. The diagrams for this process can be divided into four groups as is indicated schematically in Fig. 4. The circle means any complex diagram of $n=n'-d$ corners. The cross indicates that the external field acts before (case a), after (case b), or during (cases c and d) the emission and absorption of the virtual photons. In case c the external field acts on the meson line which passes through the diagram, in case d it acts on a closed loop. Assume that in some way we eliminated all divergencies from the meson self-energy diagrams resulting from Fig. 4 when the external field is omitted. For Fig. 4d this diagram is identically zero, because of the odd-cornered loop. Figure 4d is therefore to be understood as containing all meson self-energy diagrams to which a closed loop is connected by one or more photon lines in such a way that the order of the total diagram is the same as that of the other diagrams of Fig. 4. The action of the external field will modify our integrals in such a way that they will all diverge; for example Fig. 4a will yield the expression

$$\phi^*(p^1)1/((p^1)^2+m^2)(p_\mu{}^1+p_\mu{}^2)A_\mu{}^e(p^1-p^2)\phi(p^2) \tag{45}$$

which is singular, since p^1 satisfies $(p^1)^2+m^2=0$.

Equation (41) permits us to separate the infinite parts of (45) unambiguously, as will be described later. These infinite parts will be called "wave function renormalization" (cases a and b), "spurious charge renormalization" (case c), and "true charge renormalization" (case d) (see Fig. 4). For reasons which will become clear in the following we shall refer to all infinities arising from closed loops as "true charge renormalization." As is shown in Appendix I, the wave function renormalization and the spurious charge renormalization cancel identically to every order n'. In the next section this will be verified to lowest order ($n'=2$) by direct calculation.—The only remaining charge renormalizations of the processes of type (3) are therefore the "true" charge renormalizations, i.e., those which arise from the action of external fields on closed loops (Fig. 4d).

Consider next the radiative corrections of order n' of the Compton effect and related phenomena [type (5)]. These diagrams can again be separated into several groups as shown in Fig. 5 for the scattering of an electron by an external field to second order in this field. Figures 5a and b are all the meson scattering diagrams of Fig. 4 preceded and followed by a scattering. Figures 5c and d are all the meson self-energy diagrams of order n' preceded and followed by a double scattering in a double corner. Figures 5e, f, and g are the diagrams in which, respectively, both, one, or none of the two external field actions occur on the through-going meson line. (Figure 5f has to be understood in an analogous way to Fig. 4d.) When they are not acting on the latter they act necessarily on closed loops.

Let us assume that all infinities have been removed from the radiative corrections of order n' to the meson self-energy and to the scattering of an electron by an external field to *first* order in that field as was described before. Those diagrams of Figs. 5a and b which are derived from Figs. 4a, b, and c by an additional scattering will not give divergencies, since they will result in expressions of the form

$$\phi^*(p^1)(2p_\mu{}^1-q_\mu)A_\mu{}^e(q)1/[(p^1-q)^2+m^2] (p_\nu{}^1+p_\nu{}^2-q_\nu)A_\nu{}^e(p^1-p^2-q), \tag{46}$$

which are not singular as (45), due to the equations of motion. The other diagrams in the group Figs. 5a and b —derived from Fig. 4d—will give wave function renormalizations which exactly cancel the spurious charge renormalizations of Fig. 5f, for these divergencies will be of the same form as those of Fig. 4. On the other hand, the double corners added to the meson self-

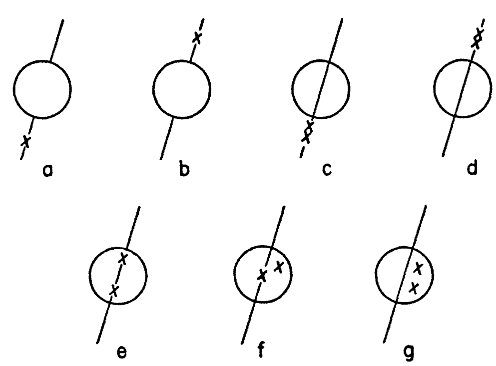

FIG. 5. The meson scattering diagrams to second order in the external field. If the crosses are replaced by photon lines these diagrams represent the Compton effect.

the physical results of quantum electrodynamics, but not always for meson theory. Since the introduction of such conditions is quite arbitrary, physical results will remain unaffected only if the divergence is a mass or charge normalization. They can therefore safely be introduced in the case of spin ½, but for the spin 0 case discussed here it would determine arbitrarily the amount of direct meson-meson interaction which is experimentally observable (see Section VI). An experimental check on this procedure is therefore possible.

energies in Figs. 5*c* and *d* again give rise to terms similar to (45), i.e.,

$$\phi^*(p^1)1/[(p^1)^2+m^2]A_\mu{}^e(q)A_\mu{}^e(p^1-p^2-q)\phi(p^2). \quad (45)$$

As before, this wave function renormalization will exactly cancel the spurious charge renormalization of Fig. 5*e*. Again, the only remaining charge renormalization will arise from the action of $A_\mu{}^e$ on closed loops (Fig. 5*g*). This will be verified by direct calculation to lowest order ($n'=2$) in the next section, but is true to all orders as proven in Appendix I. Corresponding arguments hold for the other processes of type 5 in which one or both $A_\mu{}^e$ are replaced by A_μ.

We see, therefore, that all "true" charge renormalizations arise from closed loops only. But we have seen before that all closed loops with an odd number of single corners (or closed loops resulting from these by shrinkage) contribute an identically vanishing factor to the integrals. For all other closed loops (which may be *part* of a diagram) the only terms which could give rise to charge renormalization [see Eq. (41)] vanish identically as was seen for the case of four corners. The only exceptions are: (1) the closed loops with two "external lines," i.e., with only two lines connecting to the other part of the diagram, and (2) the closed loops with one cross and one line connecting to the other part of the diagram. These two diagram parts may be thought of as the virtual occurrence of the processes of type 2 of our list of primitive divergences, i.e., photon self-energy parts and vacuum-polarization parts. It follows that *no primitive divergent diagram other than of type (2) can contain true charge renormalizations.*

We summarize these considerations: When the spurious infinities (spurious charge renormalization and wave function renormalization) are separated properly they will cancel identically, such that the only infinities which still have to be removed from the S matrix are those arising from diagrams (or diagram parts) of type (1), (2), and (6). These are the infinities associated with mass, charge, and direct interaction.

B. Separation of Divergencies

Most diagrams do not satisfy the condition that their integrals converge if any one of the internal momenta is held fixed. They will have more divergent terms in the expansion (41) than the primitive divergents of the same process. Such diagrams are called "reducible." They will contain primitive divergent parts of the types (1) to (6). We further distinguish between "proper" and "improper" diagrams, the latter being diagrams which can be separated into two unconnected diagrams by cutting only one internal line. Primitive divergent diagrams are proper, but not *vice versa.*

Consider the integral

$$\int R(p,t)d_4t \quad (47)$$

over all internal momenta, where $R(p,t)$ is defined as

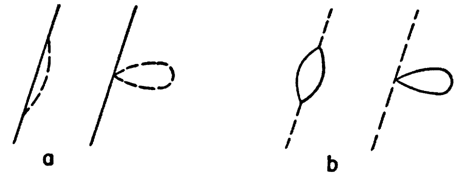

FIG. 6. The only primitive divergent self-energy diagrams. *a*: Meson self-energy. *b*: Photon self-energy.

in (41) but does not necessarily refer to a primitive divergent diagram. The integral (47) for the radiative corrections of order n' of the processes of type (1) to (6) [except (4)] will be denoted, respectively, by

$$\Sigma^{(n')}(p),\quad \Pi^{(n')}(k),\quad \Lambda_\mu{}^{(n')}(p^1,p^2),$$
$$\Omega_{\mu\nu}{}^{(n')}(p^1,p^2,k),\quad \Xi^{(n')}(p^1,p^2,p^3). \quad (48)$$

They may occur as virtual or as real processes. Where they refer to proper diagrams a star is added; the sum over all n' is indicated by omission of the superscript (n'), i.e., $\Sigma^*(p)$ is the sum over all proper self-energy diagrams. A left superscript p indicates that the proper diagram is primitive divergent.

Let $S(p)=(p^2+m^2)^{-1}$ and $D(k)=(k^2)^{-1}$ be the propagation functions of the mesons and photons. If we insert all possible radiative corrections into a meson line and sum them, we replace $S(p)$ in the integral by

$$S'(p)=S(p)+S(p)\Sigma(p)S(p)$$
$$=S(p)+S(p)\Sigma^*(p)S'(p). \quad (49a)$$

Similarly

$$D'(k)=D(k)+D(k)\Pi^*(k)D'(k). \quad (49b)$$

In order to write similar equations for $\Omega_{\mu\nu}$ and Ξ one must limit the definition of "proper diagrams" as follows. A proper "Compton effect" diagram [generally: diagram of type (5)] is one that is not only proper in the above-mentioned sense but also cannot be split into two Compton effect diagrams by cutting one meson line and one photon line. Similarly, a proper meson-meson interaction diagram is not only proper in the above sense but also cannot be split into two meson-meson interaction diagrams by cutting two meson lines. With these definitions of "proper" one finds

$$\Omega_{\mu\nu}(p^1,p^2,k)=\Omega_{\mu\nu}{}^*(p^1,p^2,k)+\int\Omega_{\mu\lambda}{}^*(p^1,t,k)S(t)$$
$$\times D(p^1+t+k)\Omega_{\lambda\nu}(t,p^2,p^1+t+k)d_4t \quad (49c)$$

and

$$\Xi(p^1,p^2,p^3)=\Xi^*(p^1,p^2,p^3)+\int\Xi^*(p^1,p^2,t)S(t)$$
$$\times S(p^1+p^2+t)\Xi(t,p^1+p^2+t,p^3)d_4t. \quad (49d)$$

When (48) refers to primitive divergents the separation (41) yields unambiguously:

$${}^p\Sigma^{(n')}(p)=e^{n'}[A^{(n')}+B^{(n')}S^{-1}(p)$$
$$+S^{-1}(p)S_c{}^{(n')}(p)], \quad (50a)$$

$$^{p}\Pi^{(n')}(k)=e^{n'}[C^{(n')}D^{-1}(k)+D^{-1}(k)D_c^{(n')}(k)], \quad (50b)$$

$$^{p}\Lambda_\mu^{(n')}(p^1,p^2)=e^{n'}[L^{(n')}(p_\mu^1+p_\mu^2)+L_{\mu c}^{(n')}(p^1,p^2)], \quad (50c)$$

$$^{p}\Omega_{\mu\nu}^{(n')}(p^1,p^2,k)=e^{n'}[O^{(n')}\delta_{\mu\nu}+O_{\mu\nu c}^{(n')}(p^1,p^2,k)], \quad (50d)$$

$$^{p}\Xi^{(n')}(p^1,p^2,p^3)=e^{n'}[X^{(n')}+R^{(n')}(p^1,p^2,p^3)+M_c^{(n')}(p^1,p^2,p^3)]. \quad (50e)$$

The term $R^{(n')}$ in (50e) will be explained in Section VI. The constants $A^{(n')}$, $B^{(n')}$, $C^{(n')}$, $L^{(n')}$, $O^{(n')}$, and $X^{(n')}$ are finite but cut-off dependent, and are "regulated" logarithmically divergent integrals. All divergencies higher than logarithmic are put equal to zero by the use of regulators.[24] $B^{(n')}$ is the "wave function renormalization," $L^{(n')}$ and $O^{(n')}$ are the "spurious charge renormalizations." As was explained before, they cancel identically (see Appendix I) such that

$$-B^{(n')}=L^{(n')}=O^{(n')}. \quad (51)$$

We are therefore effectively left with the primitive divergents $^{p}\Sigma$, $^{p}\Pi$, and $^{p}\Xi$. It should be mentioned at this point that the only primitive divergent $^{p}\Sigma$ and $^{p}\Pi$ are those shown in Fig. 6.

The convergent parts of (50) are defined as follows:

$$S_c^{(n')}(p)=0 \text{ for } p^2+m^2=0, \quad (52a)$$

$$D_c^{(n')}(k)=0 \text{ for } k^2=0 \quad (52b)$$

$$L_{\mu c}^{(n')}(p^1,p^2)=0 \text{ for } p^1=p^2 \text{ and } (p^1)^2+m^2=0 \quad (52c)$$

$$O_{\mu\nu}^{(n')}(p^1,p^2,k)=0 \text{ for } k=0 \text{ (gauge invariance)} \quad (52d)$$

$$M_c^{(n')}(p^1,p^2,p^3)=0 \text{ for } \mathbf{p}^1=\mathbf{p}^2=\mathbf{p}^3=0,\quad (p^1)^2=(p^2)^2=(p^3)^2=-m^2. \quad (52e)$$

For a discussion of (50e) and (52e) see Section VI.

All convergent functions thus defined increase at most as a power of the logarithm for large values of the arguments, except $L_{\mu c}$ which increases linearly (times a power of the logarithm). Their effect is therefore to "smear out" the propagation functions S and D, and the corner functions $p_\mu+p_\mu'$ and $\delta_{\mu\nu}$. Similarly M_c could be regarded as a smearing out of a direct (δ-function) interaction between two mesons. (See also Appendix II.)

We can now define an unambiguous method for the separation of all infinities from any diagram. We first adopt as a "hierarchy" of divergencies the list of Section III. Any primitive divergence higher on the list has preference in separation from any lower one. However, the succession of the divergencies of type (1) and (2) may be interchanged.

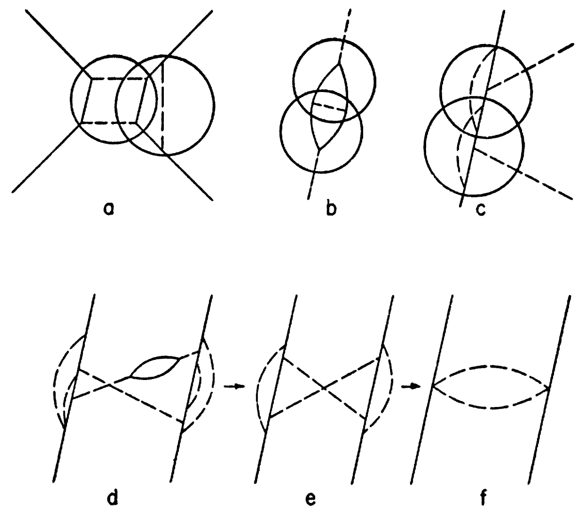

FIG. 7. Diagrams *a*, *b*, and *c* are examples of ambiguity in reduction. *b* and *c* are *b*-divergencies. Diagrams *e* and *f* illustrate the successive steps in the reduction of diagram *d*.

Every reducible diagram of a given order contains proper irreducible, and therefore at most primitively divergent, parts. The divergencies of these primitive divergent parts are to be separated according to (50). The divergent parts are then to be dropped. This separation is indicated in the diagram as follows: The replacement of $^{p}\Sigma^{(n')}(p)$ by $e^{n'}(p^2+m^2)S_c^{(n')}(p)$ in the integral is indicated by replacing the self-energy part $S(p)^{p}\Sigma^{(n')}(p)S(p)$ in the diagram by an effective meson line $e^{n'}S(p)S_c^{(n')}(p)$. (See also Appendix II.) Similarly a photon self-energy part $D(k)^{p}\Pi^{(n')}(k)D(k)$ is replaced by an effective photon line $e^{n'}D(k)D_c^{(n')}(k)$. The replacement of the primitive divergent parts of type (3), (5), and (6) by their finite parts is indicated in a diagram by replacing these parts by effective corners: type (3) will give an effective single corner, type (5) an effective double corner, and type (6) a direct interaction corner, where four meson lines meet.

This procedure would carry through without difficulty were it not for the fact that some primitive divergent parts may "overlap" as shown in Fig. 7; i.e., that they may have one or more lines in common. If two primitives of different types overlap (Fig. 7*a*), the hierarchy decides in which part the divergencies are to be separated out first. If the two primitives are of the same type (Figs. 7*b* and *c*) we are faced with the so-called *b*-divergencies. Dyson has shown how to proceed in this case (**II**, p. 1749); i.e., the divergencies of each of the two parts are to be separated out. Any ambiguities which may arise in this connection are eliminated in our case by the use of regulators.

In this way one obtains diagrams which may again contain primitive divergent parts. Some of these parts may contain effective single and double corners and effective lines. These are to be treated as "ordinary" single and double corners, and "ordinary" lines. Their divergence properties will be the same as those of "ordinary" primitive divergencies (see Appendix II); they differ from them at most by the power of a logarithm as mentioned before. Therefore, this reduction procedure can be continued until the diagram becomes irreducible, i.e., it becomes either an improper diagram whose proper parts are at most primitive divergent, or it becomes a proper irreducible diagram which is also at most primitive divergent. The last separation if necessary, is then completed and a finite result is obtained. An example of such a reduction is indicated in Figs. 7*d*, *e*, *f*.

Suppose that all integrations over the internal photon lines have been carried out and the reduced diagram consists of proper parts which contain only internal *meson* lines. Any such part which does not contain corners coupling to photons or external fields involves necessarily only "direct interaction corners." Let us investigate the possible primitive divergencies in such a diagram. With the notation of Section III we find with $D_e=0$, $E_i=f_i=0$,

$$F=F_s=2n-E_s/2,$$
$$D_{\mathrm{num}}=0,\quad D_{\mathrm{den}}=2F,$$
$$E_s\geqslant 5.$$

Since E_s is obviously even, the two primitive divergent processes are those with $E_s=2$ (quadratic) and $E_s=4$ (logarithmic). They are shown in Figs. 8*a* and *b*. All other divergent diagrams contain these as parts. For example, the diagram Fig. 8*c* contains two primitive divergencies of type Fig. 8*b*. Possible action of external fields or photons will clearly improve the order of divergence by one each, such that in general

$$E_s+E_i+f_i=E\geqslant 5,$$

which is identical with (40). We have thus shown that the introduction of direct interaction corners by the reduction procedure will yield "effective" diagrams of the same type and divergence properties as the original diagrams. Thus, by counting the external lines Figs. 8*a* and *b* are identified as primitive self-energy and meson-meson interaction which diverge exactly as the original processes. Their divergencies are to be separated out as in (50).

In this way we split the S matrix into a finite and an infinite (i.e., cut-off dependent) part in an unambiguous way. The infinite part is to be dropped. We shall now justify the omission of the infinite part by showing that these parts are equivalent to infinite factors which can be consistently incorporated into the finite parts in such a way that they constitute renormalizations of the constants originally entering the theory: The mass and charge of the mesons and the constant of direct interaction. The latter which has not entered into the theory as developed so far, has to be introduced in order to justify the omission of the terms arising from X in (50e).

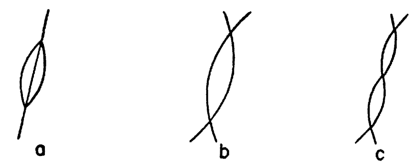

FIG. 8. Typical diagrams resulting from direct meson-meson interaction. *a*: primitive divergent meson self-energy. *b*: Primitive divergent meson-meson scattering. *c*: Reducible meson-meson scattering.

C. Removal of the Divergencies by Renormalization

The meson mass m entering the Klein-Gordon equation is the "mechanical" mass and can be written $m_1-\delta m$ where m_1 is the observed and δm the electromagnetic mass. The term $-\delta m$ will always appear together with the self-energy term Σ^*, such that (49a) becomes

$$S'(p)=S(p)+S(p)(\Sigma^*(p)-\delta m)S'(p). \tag{54a}$$

When the divergent parts of the effective meson line function $S'(p)$ are dropped, one is left with the finite function S_1'. Following Dyson we set out to prove that

$$S'=Z_2S_1'(e_1), \tag{53a}$$

where e_1 is the renormalized (observed) charge and Z_2 is an infinite constant. Similarly it should be possible to write the finite effective photon propagation function $D_1'(e_1)$ obtained by dropping the divergent terms in D' of (49b) as

$$D'=Z_3D_1'(e_1). \tag{53b}$$

Radiative corrections to a given diagram can be obtained not only by inserting corrections into the meson and photon lines S and D but also by inserting single-corner parts, i.e. diagrams of type Figs. 4*c* and *d* into single corners $C_\mu=p_\mu+p_\mu'$, and Compton effect diagrams (Figs. 5*e*, *f*, *g*) into double corners $C_{\mu\nu}=\delta_{\mu\nu}$. Making such insertions to all orders will amount to a replacement of C_μ by C_μ' and of $C_{\mu\nu}$ by $C_{\mu\nu}'$ where according to (49c)

$$C_\mu=C_\mu+\Lambda_\mu, \tag{54b}$$

$$C_{\mu\nu}'=C_{\mu\nu}+\Omega_{\mu\nu}^*+\int(C_{\mu\lambda}+\Omega_{\mu\lambda}^*)S'D'C_{\lambda\nu}. \tag{54c}$$

It is important that $\Omega_{\mu\nu}^*$ are the proper Compton diagrams as defined preceding to Eq. (49c) and do not contain diagrams followed (or preceded) by emission (or absorption), i.e., Figs. 5*a*–*d*. These diagrams would otherwise be counted twice.

When the divergent parts of these functions are dropped one obtains $C_{\mu1}'$ and $C_{\mu\nu1}'$. Their relation to the functions (54) should be

$$C_\mu'=Z_1^{-1}C_{\mu1}'(e_1), \tag{53c}$$

$$C_{\mu\nu}'=Z_4^{-1}C_{\mu\nu1}'(e_1). \tag{53d}$$

Finally radiative corrections can be obtained by replacing a direct interaction corner M by all meson-meson interaction diagrams. For this purpose we assume first that there exists a direct interaction term

$$\lambda\phi^*(x)\phi^*(x)\phi(x)\phi(x) \tag{55}$$

in the Lagrangian of our theory. Such a term would then appear additive to the interaction Hamiltonian (2). λ is an infinite constant. It is completely within the philosophy of the present theory to renormalize this coupling constant λ, since also the coupling constant e is being renormalized; thus we put $\lambda=\lambda_1-\delta\lambda$ where λ_1 is finite and is to be determined from experiment.

It follows from (49d) that each direct interaction corner M which is replaced by all possible meson-meson interactions to yield M' can be written

$$M'=\lambda_1-\delta\lambda+\Xi^*+\int(\lambda_1-\delta\lambda+\Xi^*)S'S'M'. \tag{54d}$$

When the divergent parts are dropped it gives $M_1'(e_1)$. One should thus obtain the renormalization of M' which for $\lambda_1=0$ is of the form

$$M'=Z_5^{-2}M_1'(e_1). \tag{53e}$$

The finite functions S_1', D_1', $C_{\mu 1}'$, $C_{\mu\nu 1}'$, and M_1' are well determined by the reduction procedure given in (B). It is therefore only a question of the structure of the diagrams whether or not Eqs. (53) can be fulfilled by proper choice of δm, $\delta e=e_1-e$, and $\delta\lambda$. Since Eqs. (53) are interdependent but should reproduce themselves upon insertion into each other, this procedure will prove the consistency of the renormalization program.

Consider any single-corner diagram $\Delta^{(n')}$ of order n'. Replace all lines and corners by the completely corrected lines and corners (i.e., S by S', D by D', etc.) and find $\Delta'^{(n')}$. Consider now the first radiative correction to the original diagram, $\Delta^{(n'+2)}$. It can be obtained by inserting a photon line between two meson lines thereby increasing the number of S functions by two, the number of D functions by one and the number of C_μ functions by two. It will also add a factor e^2 to the integral. We now again make the replacement $S\rightarrow S'$, $D\rightarrow D'$, $C\rightarrow C_\mu'$, etc. and find $\Delta'^{(n+2)}$. When Eqs. (53) are applied to $\Delta'^{(n')}$ and $\Delta'^{(n'+2)}$ they should result in the finite renormalized diagrams $\Delta'^{(n')}(e_1)$ and $\Delta'^{(n'+2)}(e_1)$. This is only possible consistently if the additional factor in $\Delta'^{(n'+2)}$, i.e.,

$$e^2S'S'D'C_\mu'C_\nu'=e_1^2S_1'D_1'C_{\mu 1}'C_{\nu 1}',$$

or with (53)

$$e^2_1=Z_2^2Z_3Z_1^{-2}e^2. \tag{56}$$

It is clear that the photon line inserted into $\Delta^{(n')}$ could have both ends in the same double corner. This would add instead the factor $e^2S'D'C_{\mu\nu}'=e_1^2S_1'D_1'C_{\mu\nu 1}'$ by the same argument as before

$$e_1^2=Z_2Z_3Z_4^{-1}e^2. \tag{57}$$

Equation (56) and (57) are compatible if and only if

$$Z_4=Z_1^2Z_2^{-1}. \tag{58}$$

One can now proceed just as in **II**. From Fig. 6*a* we see that Σ^* consists of one S function, one D function, two C_μ, and a factor e^2. Replacement by the primed functions and use of (53) and (56) gives $\Sigma^*-Z_2^{-1}\Sigma^*(e_1)$. Therefore (54a) with the separation (50a) yields

$$S'=S+Z_2^{-1}(SA(e_1)+B(e_1)+S_c(e_1))S'-\delta mSS'$$

which should reduce to its finite part

$$S_1'(e_1)=S+S_c(e_1)S_1'(e_1)$$

due to the renormalization (53a). This is indeed the case provided

$$\delta mZ_2=A(e_1) \tag{59}$$

and

$$Z_2=1+B(e_1). \tag{60}$$

In the same way, the structure of Fig. 6*b* leads to $\Pi^*=Z_3^{-1}\Pi^*(e_1)$ and (49b) becomes with (50b)

$$D'=D+Z_3^{-1}(C(e_1)+D_c(e_1))D'.$$

This reduces to

$$D_1'(e_1)=D+D_c(e_1)D_1'(e_1)$$

due to (53b) provided

$$Z_3=1+C(e_1). \tag{61}$$

For the renormalization of C_μ we see from (56) and Fig. 10 that $\Lambda_\mu=Z_1^{-1}\Lambda_\mu(e_1)$ such that (54b) with the separation (50c) becomes

$$C_\mu'=C_\mu+Z_1^{-1}(C_\mu L(e_1)+L_{\mu c}(e_1))$$

which reduces to its finite part

$$C_{\mu 1}'(e_1)=C_\mu+L_{\mu c}(e_1)$$

due to (53c) provided

$$Z_1=1-L(e_1). \tag{62}$$

As is proved in Appendix I [Eq. (A11)] $B+L=0$, since it is true in each order. Therefore (60), (62), and (58) give at once

$$Z_1=Z_2=Z_4, \tag{63}$$

and (56) simplies to

$$e_1^2=Z_3e^2=(1+C(e_1^2))e^2. \tag{56'}$$

Equation (63) is another statement of the cancellation of spurious charge and wave function renormalization. This cancellation occurs explicitly in Eq. (56) such that the complete "true" charge renormalization is due only to the renormalization of D' of (53b). Since any insertions into the D lines always reduce to effective diagrams of the form Fig. 6*b*, we find again that only closed loops with two single corners or one double corner yield charge renormalization.

We also observe that Z_4 the renormalization associated with the Compton effect diagrams is already determined by Z_1 and Z_2 which is actually a consequence of gauge invariance (see the remark at the end of Appendix I).

The above analysis which resulted in the determination of the Z_i in terms of the infinite integrals can, of course, in principle be continued for $C_{\mu\nu}'$ and M'. This would result, of course, in the same equations as above. From Fig. 11 and Eq. (56) one finds

$$\Omega_{\mu\nu}^* = Z_2 Z_1^{-2} \Omega_{\mu\nu}^*(e_1).$$

The renormalization of S' and D' in the integral (54c), observing that there are two more factors of e to be renormalized (one of the "external" charges of each diagram connected by D') yields

$$C_{\mu\nu}' = C_{\mu\nu} + Z_2 Z_1^{-2} \Omega_{\mu\nu}^*(e_1)$$
$$+ Z_1^2 Z_2 \int (C_{\mu\lambda} + Z_2 Z_1^{-2} \Omega_{\mu\lambda}^*(e_1)) S'(e_1) D'(e_1) C_{\lambda\nu}'. \quad (64)$$

This should reduce to $C_{\mu\nu 1}'(e_1)$ due to (53d). However, the analysis cannot be carried further, because $C_{\mu\nu 1}'(e_1)$ is not known in closed form. Although it is uniquely determined by the reduction prescription, it is not possible to write down its form. This is already indicated by the fact that the integral in (64) diverges even if the factors of the integrand are replaced by their finite parts. The reason for this apparently unexpected divergence is to be found in the b-divergences of the type shown in Fig. 7c. Whenever these diagrams occur the separation into proper diagrams of type (5) (Compton effect, etc.) becomes ambiguous. Of course, it is irrelevant which separation is chosen, but it is due to this ambiguity that the separation of the infinite parts of the two diagrams of type (5) thus obtained does not completely separate out all infinite terms. Since the integral in (64) is just based on this separation one cannot expect it to be finite. On the other hand, only some of the improper diagrams of type (5) will contain b-divergencies; it will therefore not be possible to write down a closed analytic expression correct for all cases.

One may argue that the renormalization procedure has to be consistent even if one restricts $C_{\mu\nu}'$ to proper diagrams omitting the integral in (64). One finds in this case from (50d)

$$C_{\mu\nu}' = C_{\mu\nu} + Z_2 Z_1^{-2} (O(e_1) C_{\mu\nu} + O_{\mu\nu}(e_1))$$

which reduces to

$$C_{\mu\nu 1}'(e_1) = C_{\mu\nu} + O_{\mu\nu}(e_1)$$

due to (53d) provided

$$Z_4 = 1 - O(e_1) \quad (65)$$

and Eq. (58) holds. Equations (66) and (62) combined with the result of Appendix I (A12) confirm $Z_2 = Z_4$ found previously [Eq. (65)].

Finally we turn to the meson-meson interaction and observe that the same difficulty encountered in the integral of (54c) is also present in (54d). The case is completely analogous to the one discussed above. If we restrict ourselves to $\lambda_1 = 0$ and to proper Ξ, one finds from Fig. 12 that $\Xi^* = Z_2^{-2} \Xi^*(e_1)$. Therefore, with (50e)

$$M' = -\delta\lambda + Z_2^{-2}(X(e_1) + M_c(e_1) + R(e_1))$$

which reduces to

$$M_1'(e_1) = M_c(e_1) + R(e_1)$$

due to (53e) provided that

$$\delta\lambda = Z_2^{-2} X(e_1) \quad (66)$$

and that

$$Z_5 = Z_2. \quad (67)$$

We have so far restricted ourselves to $\lambda_1 = 0$ in (54d). For this case the discussion of this section shows the consistency of the removal of all divergencies by renormalization. If $\lambda_1 \neq 0$ two additional types of divergencies arise. First, the divergencies due to the direct interaction term λ_1 itself which gives rise to divergent diagrams like those of Fig. 8. They can be separated into a finite part and an infinite part analogous to (50e). The latter must be canceled by a renormalization $\delta\lambda_1$ which is independent of e_1.

Second, there are radiative corrections of diagrams like Fig. 8. They diverge exactly like the effective diagrams encountered previously where the direct interaction corner was due to Ξ rather than (55). Their separation according to (50) of infinite and finite parts will result in infinite parts which depend on e_1 and on λ_1. These have to be canceled by a term $\delta\lambda_{1e}$.

We thus find that if $\lambda_1 \neq 0$, $\delta\lambda = \delta\lambda_1 + \delta\lambda_{1e} + \delta\lambda_e$, where $\delta\lambda_e$ is independent of λ_1 and is determined by (66). Since the reduction procedure uniquely separates the infinite parts which in turn define $\delta\lambda$, this quantity is well defined. The finite scattering matrix will then be a well-defined function of λ_1 and will be given as a power series in λ_1.

Before we turn to a discussion of the physical meaning and determination of λ_1 (Section VI), we shall give some examples which illustrate some of the results obtained so far.

V. THE PRIMITIVE DIVERGENT PROCESSES TO LOWEST ORDER

The second-order meson self-energy and vacuum polarization have been treated repeatedly by various authors. There is no need to give these calculations here.

A. Scattering of Light by Light

There are three kinds of diagrams, corresponding to the number of double corners (Fig. 9). From (30′) we see that they will all be of the form

$$(e/4\pi^2)^4 A_\mu(k^1) A_\nu(k^2) A_\lambda(k^3) A_\sigma(k^4)$$
$$\times T_{\mu\nu\lambda\sigma}(k^1, k^2, k^3, k^4) \delta(k^1+k^2+k^3+k^4).$$

The diagram Fig. 9*a* gives with regulators

$$T_{\mu\nu\lambda\sigma}{}^{(a)}(1234)=\Sigma c_i\int\frac{(2p_\mu-k_\mu{}^1)(2p_\nu-2k_\nu{}^1-k_\nu{}^2)(2p_\lambda-2k_\lambda{}^1-k_\lambda{}^3)(2p_\sigma+k_\sigma{}^4)d_4p}{[p^2+m_i{}^2][(p-k^1)^2+m_i{}^2][(p-k^1-k^2)^2+m_i{}^2][(p+k^4)^2+m_i{}^2]}.$$

We introduce auxiliary variables[25] and combine the denominator to give the fourth power of a quadratic form. On shifting the origin of the p space the divergent part of the integral is found to be [see Eq. (41)]

$$T_{\mu\nu\lambda\sigma}{}^{(a)}=\Sigma c_i 3!\int_0^1 dx\int_0^x dy\int^y dz\frac{16p_\mu p_\nu p_\lambda p_\sigma d_4p}{(p^2+m_i{}^2)^4}.$$

The integral vanishes unless the μ, ν, λ, σ are equal in pairs. One finds that $p_\mu p_\nu p_\lambda p_\sigma$ in the integral can be replaced by

$$(1/24)(\delta_{\mu\nu}\delta_{\lambda\sigma}+\delta_{\mu\lambda}\delta_{\nu\sigma}+\delta_{\mu\sigma}\delta_{\nu\lambda})p^2p^2$$

and the integration can be carried out over four-dimensional spherical coordinates with volume element $2\pi^2p^3dp$ as explained in **II**. One finds

$$T_{\mu\nu\lambda\sigma}{}^{(a)}=(16/24)2\pi^2 i(\delta_{\mu\nu}\delta_{\lambda\sigma}+\delta_{\mu\lambda}\delta_{\nu\sigma}+\delta_{\mu\sigma}\delta_{\nu\lambda})\times\Sigma c_i\tfrac{1}{2}\ln(M_c{}^2/m_i{}^2)\equiv\tfrac{2}{3}Q_{\mu\nu\lambda\sigma},$$

where M_c is an upper cut-off mass. The relation $\Sigma c_i=0$ was used. There are 24 permutations of the four corners in Fig. 9*a* which can be obtained from six of them by cyclic permutations. Therefore there are six diagrams of the type Fig. 9*a* which need to be taken into account. These six are 1234, 1324, 1243, and their "charge—conjugates," obtained by reversing the sense of all the arrows, i.e., 4321, 4231, 3421. The latter three are identical with the former three by Furry's theorem. Since $T_{\mu\nu\lambda\sigma}{}^{(a)}$ is invariant under the concomitant permutation of 1234 and $\mu\nu\lambda\sigma$, we find for the sum of divergent parts of the three essentially different diagrams of the form Fig. 9*a*

$$\Sigma T_{\mu\nu\lambda\sigma}{}^{(a)}=2Q_{\mu\nu\lambda\sigma}.$$

Each of these three diagrams gives four diagrams of type Fig. 9*b* by shrinkage of the meson lines. The one actually drawn gives

$$T_{\mu\nu\lambda\sigma}{}^{(b)}(1234)=\Sigma c_i\int(-\delta_{\mu\sigma})\times\frac{(2p_\nu-2k_\nu{}^1-k_\nu{}^2)(2p_\lambda-2k_\lambda{}^1-2k_\lambda{}^2-k_\lambda{}^3)d_4p}{(p^2+m_i{}^2)[(p-k^1)^2+m_i{}^2][(p-k^1-k^2)^2+m_i{}^2]}.$$

As before one finds, since $p_\nu p_\lambda$ can be replaced by $\frac{1}{4}\delta_{\nu\lambda}p^2$,

$$T_{\mu\nu\lambda\sigma}{}^{(b)}=2!\int_0^1 dx\int_0^x dy\Sigma c_i\frac{4p_\nu p_\lambda d_4p}{(p^2+m_i{}^2)^3}\delta_{\mu\sigma}=-i\pi^2\delta_{\mu\sigma}\delta_{\nu\lambda}\Sigma c_i\ln(Mc^2/m_i{}^2).$$

The three other ways of shrinkage of 1234 will give the same result with $\delta_{\mu\sigma}\delta_{\lambda\nu}$ replaced by $\delta_{\mu\nu}\delta_{\lambda\sigma}$, $\delta_{\nu\lambda}\delta_{\mu\sigma}$, and $\delta_{\lambda\sigma}\delta_{\mu\nu}$, respectively. The sum of all diagrams Fig. 9*b*, resulting from 1234 is therefore

$$-2\pi^2 i(\delta_{\mu\sigma}\delta_{\nu\lambda}+\delta_{\mu\nu}\delta_{\lambda\sigma})\Sigma c_i\ln(M_c{}^2/m_i{}^2).$$

The results from shrinkage of 1324 are obtained from this by replacing μ, ν, λ, σ by μ, λ, ν, σ, respectively, yielding

$$-2\pi^2 i(\delta_{\mu\sigma}\delta_{\nu\lambda}+\delta_{\mu\lambda}\delta_{\nu\sigma})\Sigma c_i\ln(M_c{}^2/m_i{}^2)$$

and similarly from 1243, replacing μ, ν, λ, σ instead by μ, ν, σ, λ,

$$-2\pi^2 i(\delta_{\mu\lambda}\delta_{\nu\sigma}+\delta_{\mu\nu}\delta_{\lambda\sigma})\Sigma c_i\ln(M_c{}^2/m_i{}^2).$$

Therefore,

$$\Sigma T_{\mu\nu\lambda\sigma}{}^{(b)}=-4Q_{\mu\nu\lambda\sigma}.$$

The same result could have been obtained by drawing all diagrams of type Fig. 9*b* and multiplying by the weight factor 2.

Each of the diagrams of the type Fig. 9*b* can be shrunk once to yield a diagram of Fig. 9*c*. The one drawn is

$$T_{\mu\nu\lambda\sigma}{}^{(c)}(1234)=\Sigma c_i\int\frac{(-\delta_{\mu\sigma})(-\delta_{\nu\lambda})d_4p}{[(p-k')^2+m_i{}^2][p^2+m_i{}^2]},$$

$$T_{\mu\nu\lambda\sigma}{}^{(c)}=\delta_{\mu\sigma}\delta_{\nu\lambda}\Sigma c_i\int_0^1 dx\int\frac{d_4p}{(p^2+m_i{}^2)^2}=\delta_{\mu\sigma}\delta_{\nu\lambda}i\pi^2\Sigma c_i\ln(M_c{}^2/m_i{}^2).$$

The four diagrams *b* resulting from 1234 will on shrinkage give two diagrams *c* as the one just calculated and two diagrams with $\delta_{\mu\sigma}\delta_{\nu\lambda}$ replaced by $\delta_{\mu\nu}\delta_{\lambda\sigma}$. Summing again over the permutations μ, λ, ν, σ and $\mu\nu\sigma\lambda$ corresponding to the diagrams resulting from 1324 and 1243 we find

$$\sum T_{\mu\nu\lambda\sigma}{}^{(c)}=2Q_{\mu\nu\lambda\sigma}.$$

The sum of all diagrams Fig. 9 is therefore

$$\sum T_{\mu\nu\lambda\sigma}{}^{(a)}+\sum T_{\mu\nu\lambda\sigma}{}^{(b)}+\sum T_{\mu\nu\lambda\sigma}{}^{(c)}=0$$

as required by gauge invariance.

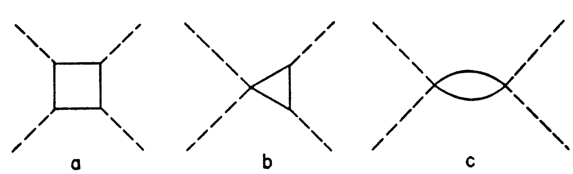

FIG. 9. The scattering of light by light in lowest order.

[25] See R. P. Feynman, reference 5, p. 785.

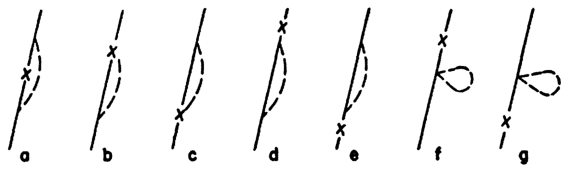

FIG. 10. Meson scattering to first order in the external field and in lowest order of correction. Note that the diagrams describing the effect of vacuum polarization were omitted here.

B. Lamb Shift and Associated Phenomena

In this process as well as in the Compton effect dealt with subsequently, we want to show how the spurious charge renormalizations and wave function renormalizations cancel. For this purpose we will content ourselves to show the cancellation of the divergent upper limit of the integrals, and we shall ignore "infrared divergencies" and finite renormalizations. In this way we shall greatly simplify the discussion, and we do not need to introduce regulators.

The diagrams are shown in Fig. 10. Apart from uninteresting constants Fig. 10a gives

$$\Lambda_\mu^{(a)}(p,p')=\int\frac{(2p_\lambda-k_\lambda)(2p_\lambda'-k_\lambda)(P_\mu+2k_\mu)d_4k}{k^2(k^2+2p\cdot k)(k^2+2p'\cdot k)},\tag{68}$$

where k is the momentum of the virtual photon, $P=p+p'$ and $p^2=p'^2=-m^2$. It is now convenient to introduce the variable $k'=k+\frac{1}{2}P$ which will enable us to eliminate the linearly divergent term correctly. One finds after putting $p=p'$

$$\Lambda_\mu^{(a)}(p,p)=\int\frac{(p+k')^2\cdot 2k_\mu' d_4k'}{(k'-p)^2(k'^2-p^2)}.$$

For large k' we can put $(k'-p)^{-2}=(1+2k\cdot p/k^2)/k'^2$. The linearly divergent term now vanishes because of symmetry and the remainder gives for large k

$$L^{(a)}p_\mu=p_\mu\int d_4k/(k^2)^2\equiv p_\mu I.$$

In the same way Figs. 10b and c give together

$$\Lambda_\mu^{(b)}(p,p')+\Lambda_\mu^{(c)}(p,p')$$
$$=2\int\left[\frac{-\delta_{\mu\nu}(2p_\nu+k_\nu)}{k^2(k^2+2p\cdot k)}+\frac{-\delta_{\mu\nu}(2p_\nu'+k_\nu)}{k^2(k^2+2p'\cdot k)}\right]d_4k,$$

where the factor 2 is the weight factor. For large k we can again put $(k^2+2p\cdot k)^{-1}=(1-2p\cdot k/k^2)/k^2$ and find

$$L^{(b)}+L^{(c)}=-3I,\quad L=L^{(a)}+L^{(b)}+L^{(c)}=-2I.\tag{69}$$

The remaining diagrams of Fig. 10 will give wave function renormalizations.

$$\Lambda_\mu^{(d)}+\Lambda_\mu^{(e)}=\tfrac{1}{2}P_\mu\int\left[\frac{(2\bar{p}-k)^2d_4k}{[(\bar{p}-k)^2+m^2]k^2(\bar{p}^2+m^2)}+\frac{(2\bar{p}'-k)^2d_4k}{[(\bar{p}'-k)^2+m^2]k^2(\bar{p}'^2+m^2)}\right],\tag{70a}$$

$$\Lambda_\mu^{(f)}+\Lambda_\mu^{(g)}=\tfrac{1}{2}P_\mu\int\left[\frac{-\delta_{\nu\nu}}{(\bar{p}^2+m^2)k^2}+\frac{-\delta_{\nu\nu}}{(\bar{p}'^2+m^2)k^2}\right]d_4k.\tag{70b}$$

From these integrals first the mass renormalization has to be subtracted, i.e., we have to subtract

$$\tfrac{1}{2}P_\mu\int\left[\frac{(2p-k)^2}{(k^2-2p\cdot k)k^2(\bar{p}^2+m^2)}+\frac{(2p'-k)^2}{(k^2-2p'-k)k^2(\bar{p}'^2+m^2)}\right]d_4k$$
$$+\tfrac{1}{2}P_\mu\int\left[\frac{-\delta_{\mu\nu}}{(\bar{p}^2+m^2)k^2}+\frac{-\delta_{\nu\nu}}{(\bar{p}'^2+m^2)k^2}\right]d_4k.\tag{71}$$

One observes that the diagrams Fig. 10f and g exactly cancel out. They do not contribute to observable effects. It can easily be seen that these double-corner self-energy terms will always behave in this manner.

$\bar{p}_\mu$ and $\bar{p}_\mu'$ of (70) obey $p^2=p'^2=-m^2$ only after (71) has been subtracted. One therefore replaces them first by $(1+\epsilon)p_\mu$ and $(1+\epsilon)p_\mu'$ and passes to the limit $\epsilon\to 0$ in the difference (70)–(71). The resultant linearly divergent integral may be treated similarly to (68) and yields after an easy calculation the wave function renormalization

$$B=2I,\tag{72}$$

which exactly cancels the spurious charge renormalization (69).

C. Compton Effect and Associated Phenomena

We will here be concerned with the radiative correction to the scattering of an electron by an external field to second order in that field. The diagrams are those of the Lamb shift (Fig. 10) preceded or followed by an additional scattering, those containing true charge renormalizations (i.e., diagrams with parts of the form Fig. 6b), and those shown in Fig. 11. The latter are special cases of Figs. 5c, d, e. The calculation is carried out as in Section B. One finds

$$\Omega_{\mu\nu}^{(a)}=\int\frac{(2p_\lambda+k_\lambda)(2p_\lambda'+k_\lambda)(2p_\mu+2k_\mu+q_\mu)(2p_\nu'+2k_\nu+q_\nu')}{k^2(k^2+2p\cdot k)[(k+q)^2-2p\cdot(k+q)](k^2+2p'\cdot k)}d_4k+(\text{same with }\mu,\nu\text{ and }q,q'\text{ interchanged})$$

which for large k_μ yields

$$O^{(a)}\delta_{\mu\nu}=2\int d_4k\cdot 4k_\mu k_\nu/(k^2)^3=2\delta_{\mu\nu}I.$$

Similarly, with weight factor 2

$$\Omega_{\mu\nu}{}^{(b)}=2\int\frac{(2p+k)\cdot(2p'-k)(-\delta_{\mu\nu})}{k^2(k^2+2p\cdot k)(k^2+2p'\cdot k)}d_4k,$$

$$O^{(b)}=-2I,$$

$$\Omega_{\mu\nu}{}^{(c)}+\Omega_{\mu\nu}{}^{(d)}=2\int\frac{(2p_\lambda+k_\lambda)(-\delta_{\lambda\nu})(2p_\mu+2k_\mu+q_\mu)d_4k}{k^2(k^2+2p\cdot k)[(k+q)^2+2p\cdot(k+q)]}$$
$$+2\int\frac{(2p_\lambda'+k_\lambda)(-\delta_{\lambda\nu})(2p_\mu'+2k_\mu+q_\mu)d_4k}{k^2(k^2+2p'\cdot k)[(k+q)^2+2p'\cdot(k+q)]}$$
$$+(\text{same with } \mu,\ \nu \text{ and } q,\ q' \text{ interchanged}),$$

$$O^{(c)}+O^{(d)}=-4I.$$

The last spurious charge renormalization diagram, Fig. 11e, has weight 4

$$O_{\mu\nu}{}^{(e)}=4\int\frac{(-\delta_{\mu\lambda})(-\delta_{\lambda\nu})d_4k}{k^2[(k+q)^2+2p\cdot(k+q)]}$$
$$+(\text{same with } \mu,\ \nu \text{ and } q,\ q' \text{ interchanged}),$$

$$O^{(e)}=8I.$$

Together they give

$$O=O^{(a)}+O^{(b)}+O^{(c)}+O^{(d)}+O^{(e)}=4I. \qquad (73)$$

The sum of the wave function renormalization diagrams, Fig. 11f and g, obviously yield the same integrals as Figs. 10d and e, except that P_μ in the latter is to be replaced by $-2\delta_{\mu\nu}$. One therefore finds at once from (70) and (72)

$$B=-4I$$

which again cancels (73).

D. Meson-Meson Scattering

The diagrams for this process to fourth order are shown in Fig. 12. The circle in Fig. 12e stands for *all* the Lamb shift diagrams with the external field replaced

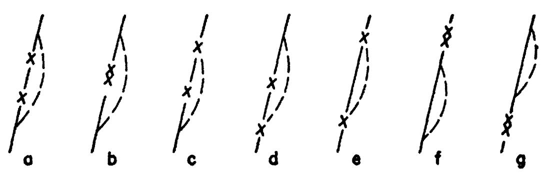

FIG. 11. Meson scattering to second order in the external field and in lowest order of correction. When the crosses are replaced by photon lines these diagrams represent the first radiative corrections to Compton scattering. Note that these are not *all* of the diagrams for these processes (see text).

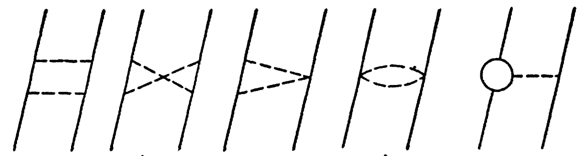

FIG. 12. The first radiative correction to meson-meson scattering. The circle in e stands for all single-corner parts in that order of correction.

by a photon line. Therefore, the sum of all diagrams e contains only true charge renormalizations. One finds, observing the weight factors:

$$\Xi^{(a)}=\int\frac{(2p^1-k)\cdot(2p^2+k)(p^1+p^3-k)\cdot(p^2+p^4+k)}{k^2(k+p^3-p^1)^2(k^2-2p^1\cdot k)(k^2+2p^2\cdot k)}d_4k,$$

$$\Xi^{(b)}=\int\frac{(2p^1-k)\cdot(2p^4-k)(p^1+p^3-k)\cdot(p^2+p^4-k)}{k^2(k+p^3-p^1)^2(k^2-2p^1\cdot k)(k^2-2p^4\cdot k)}d_4k,$$

$$\Xi^{(c)}=-2\int\frac{(2p^1-k)\cdot(p^1+p^3-k)}{k^2(k+p^3-p^1)^2(k^2-2p^1\cdot k)}d_4k$$
$$-2\int\frac{(2p^2+k)\cdot(p^2+p^4+k)}{k^2(k+p^3-p^1)^2(k^2+2p^2\cdot k)}d_4k,$$

$$\Xi^{(d)}=2\int\frac{(-\delta_{\mu\nu})(-\delta_{\nu\mu})}{k^2(k+p^3-p^1)^2}d_4k.$$

Thus, with (50e)

$$X=X^{(a)}+X^{(b)}+X^{(c)}+X^{(d)}=I+I-4I+8I=6I.$$

From this and Eq. (66) one finds $\delta\lambda$.

VI. DISCUSSION OF THE RESULTS

First, the equivalence of the Kanesawa-Tomonaga theory with the Feynman theory is established by proving the identity of the scattering matrices of the two theories. Second, the divergencies of the S matrix are investigated and an unambiguous way for the separation of the finite and infinite parts is given. Finally, all divergencies are removed by renormalization.

One finds that the quantum electrodynamics of spinless particles is in many ways similar to the one for particles of spin $\frac{1}{2}$. There are, however, these essential differences. The non-linear terms of the interaction Hamiltonian give rise to double corners in the diagrams; this in turn is closely related to the fact that both the Lamb shift diagrams and the Compton effect diagrams lead to divergencies. However. these divergencies are shown to be entirely spurious. But the divergent Compton effect diagrams give rise to a b-divergence problem which is much more complicated than the b-divergence problem in the electron case. In the latter these divergencies occur only in very special cases since they are there only associated with electron and photon self-energy diagrams of which there exist only two primitive divergent ones. In the spinless case there is an infinite number of b-divergent diagrams.

Further complication arises from the meson-meson interaction which is found to be divergent. This divergence necessitates the introduction of a direct interaction term into the Hamiltonian. It is this point which deserves further clarification.

As is well known, the long range of the Coulomb potential causes the scattering amplitude to become arbitrary large for small enough energy-momentum transfer $\Delta=p^1-p^3$. Terms of the type $1/\Delta$ arising, for example, in fourth order are physically undistinguishable from similar terms arising in second order. It is therefore satisfactory to see them arise only in connection with charge renormalization, i.e., they come from those fourth-order diagrams which are derived from Lamb shift diagrams, but not from Ξ. There are, however, corrections to the Coulomb potential at smaller distances from terms of the type $\ln\Delta$ occurring in ${}^p\Xi$. These terms have to be separated from ${}^p\Xi$ in the separation (50e) with the definition (52e) of M_c.

Consider a primitive divergent meson-meson scattering diagram ${}^p\Xi(p^1\ p^2\ p^3, p^4)$ for initial four-momenta p^1, p^2 and final four-momenta p^3, p^4 where $p^1+p^2=p^3+p^4$ because of energy-momentum conservation. Introduce regulators and photon masses, the latter to properly take into account the infra-red divergencies. The result of the various integrations will contain constant, logarithmically cut-off dependent terms X which are defined within an additive cut-off independent constant X'. One can now define a term R which is logarithmically divergent for $\Delta=p^1-p^3=0$,

$$R=r\ln(\Delta/m), \tag{74}$$

where

$$r=\lim_{\Delta\to 0}({}^p\Xi-X)/\ln(\Delta/m). \tag{75}$$

m is the meson mass. The limit is taken with p^1+p^3 and p^2+p^4 held fixed. r will be a function of these two combinations only. The finite function

$$M_c={}^p\Xi-X-R$$

is now defined within the constant X'.

This constant can be defined by defining R [e.g., as in (74)] and M_c [e.g., by choosing the definition (52e)]. The direct or contact interaction is then solely due to λ_1 which has to be found from experiment. However, we do not intend to imply that the interaction $R+M_c$ thus defined is free from contact interaction. In fact, there seems to be no simple unambiguous way of defining such a contact-free interaction.[26] The separation into contact and contact-free interaction must therefore be regarded as arbitrary. One might indeed equally well choose $\lambda_1=0$, i.e., one may renormalize λ to zero, and leave M_c undetermined within the additive constant X' which is to be determined by experiment.

I would like to thank Professors R. P. Feynman and N. M. Kroll for many helpful discussions throughout this work. The author is also grateful to Professor H. A. Bethe for his valuable criticism of the manuscript.

Note added in proof: The integrals in equations (49c and d) and therefore also in equations (54c, d) and (64) are oversimplified and consequently incorrect. However, they have not been used in the arguments so that the results and conclusions remain unaffected.—This author believes that the existence proof by construction of the finite S matrix as outlined in section VB should be supplemented by a mathematical formulation of this procedure. This would enable one to give a detailed proof of the consistency of the renormalization program (section VC). But it requires a detailed analysis of the treatment of b-divergencies; these have not been considered in this paper. Such analysis should furnish the correct integrals of (49c and d).

APPENDIX I. CANCELLATION OF SPURIOUS CHARGE RENORMALIZATION AND WAVE FUNCTION RENORMALIZATION

The proof presented here will be given in complete generality, valid for spin 0, $\frac{1}{2}$, and 1, and for the formulation with and without Kemmer-Duffin matrices in the cases of integer spin.

Let ψ be the source field and

$$S^{-1}(p)\psi=0 \tag{A1}$$

the equation of motion of the free field. $S(p)$ is the propagation function of the source particles. The coupling to the electromagnetic field $A_\mu^e(q)$ is given by the operator $C_\mu(p,p')$ where $p_\mu-p_\mu'=q_\mu$. This operator represents the single corner of a diagram, e.g., it is γ_μ for spin $\frac{1}{2}$ and it is $p_\mu+p_\mu'$ in our formulation of spin 0.

As is obvious from an expansion[27] of $S^{-1}(p-A)$,

$$C_\mu(p,p)=\partial S^{-1}(p)/\partial p_\mu. \tag{A2}$$

If (A1) is quadratic in p there will also be a quadratic term in A_μ^e with coefficient

$$C_{\mu\nu}=-\frac{1}{2}\frac{\partial^2 S^{-1}(p)}{\partial p_\mu\partial p_\nu}=-\frac{1}{2}\frac{\partial C_\mu(p,p)}{\partial p_\nu}. \tag{A3}$$

From (A2) the identity

$$-\partial S(p)/\partial p_\mu=S(p)C_\mu(p,p)S(p) \tag{A4}$$

is an immediate consequence. If p_μ satisfies (A1) we find the useful relation

$$\lim_{p_\mu'\to p_\mu} S(p')(p_\mu'-p_\mu)C_\mu(p,p)\psi=\psi. \tag{A5}$$

A proper Lamb shift diagram Λ_μ^* is obtained by inserting into a proper source particle self-energy diagram Σ^* the action of $A_\mu^e(q)$. If this is done in a source line $S(p')$, it will replace it by $S(p')C_\mu(p',p')S(p')$ for $q=0$. If it is done at a single corner it will produce a double corner with coupling function $2C_{\mu\nu}$ again for $q=0$. In all cases considered here either $C_\mu(p,p)$ is a constant and no double corner exists [$S^{-1}(p)$ is linear] or $C_{\mu\nu}$ is a constant [$S^{-1}(p)$ is quadratic]. The factor 2 which enters here in a natural way is the weight factor.

[26] Two possible definitions of a contact-free meson-meson interaction seem to be of particular interest. First, there is the analogy with the electron case in which the corresponding interaction is well defined and may be considered as not containing a direct interaction. Second, one might use regulators with the additional condition $\Sigma c_i\ln m_i=0$ for a contact free interaction. One then does not need a direct interaction term (55). The amount of contact interaction is $\Sigma c_i\ln m_i=0$ (see also footnote 24). Further investigation of these points may show that the two definitions proposed here are actually identical.

[27] The coupling of the electromagnetic field A_μ to the bare particles by replacing p_μ by $p_\mu-A_\mu$ is a requirement of gauge-invariance. Since the whole proof is based on this fact, the cancellation of the renormalizations can therefore be thought of as a consequence of gauge-invariance.

Summing over all possible insertions of $A_\mu^e(0)$ we find with (A3) and (A5),

$$\Lambda_\mu^*(p, p) = -\partial\Sigma^*(p)/\partial p_\mu. \quad (A6)$$

If Σ^* is of order n', Λ_μ^* will be of the same order. We now assume that all primitive divergent parts of lower order have been properly replaced by their finite parts, such that $\Sigma^{*(n')}$ and $\Lambda_\mu^{*(n')}$ are primitive divergent effective diagrams, i.e., they will contain effective lines and corners. Therefore, a separation of the form (50c) is possible and since $L_{\mu c}^*(p, p)\psi = 0$ by definition we find

$$e^{n'}L^{(n')}C_\mu(p, p) = -\partial\Sigma^*(p)/\partial p_\mu. \quad (A7)$$

It is to be noted here that we have not excluded the action of the electromagnetic field in closed loops, but that these contributions vanish by Furry's theorem, for the even number of corners of the loops in Σ^* becomes odd by the action of A_μ^e. Therefore (A7) gives correctly the spurious charge renormalization of the diagrams c of Fig. 4.

Repeating this insertion process we find from a separation of the form (50d) of the primitive divergent diagram of type (5) (Compton effect and related phenomena) $\Omega_{\mu\nu}^{*(n')}(p, p)$ since $O_{\mu\nu}^{*(n')}(p, p) = 0$

$$2e^{n'}O^{(n')}C_{\mu\nu} = -\partial\Lambda_\mu^{*(n')}(p, p)/\partial p_\nu = \partial^2\Sigma^{*(n')}(p)/\partial p_\mu\partial p_\nu. \quad (A8)$$

From (A5), (A7), and (A8) it follows therefore that

$$O^{(n')} = L^{(n')}. \quad (A9)$$

Clearly, if $C_{\mu\nu} = 0$, $O^{(n')}$ does not exist and the processes of type (5) are convergent. $O^{(n')}$ is the spurious charge renormalization arising from the diagrams of Fig. 5e.

Let $\Sigma^{*(n')}(p')$ be an effective, but primitive divergent diagram. Then the separation (50a) is valid and the diagrams 4a and b give

$$C_\mu(p', p')S(p')\Sigma^{*(n')}(p') = e^{n'}C_\mu(p', p')(A^{(n')}S(p) + B^{(n')} + S_c^{(n')}(p')). \quad (A10)$$

The first term will be canceled by the mass renormalization which can be written

$$e^{n'}C_\mu(p', p')S(p')\Sigma^{*(n')}(p),$$

where p_μ, in contradiction to p_μ', satisfies (A1). We subtract it from (A10) and expand $\Sigma^{*(n')}(p')$ near p. Comparing the infinite terms on both sides we find for the wave function renormalization constant

$$e^{n'}B^{(n')} = S(p')[\partial\Sigma^{*(n')}(p)/\partial p_\lambda](p_\lambda' - p_\lambda).$$

This yields with (A7) and the identity (A5) as we pass to the limit $p_\mu' \to p_\mu$

$$B^{(n')} + L^{(n')} = 0. \quad (A11)$$

Equation (A11) expresses the identical cancellation of the infinities arising from Figs. 4a, b, and c. It is to be noted that the wave function renormalization constant for each of the diagrams 4a and b is only $\frac{1}{2}B^{(n')}$ since it is associated with the outgoing source line which is shared by the next scattering process.

On calculating the wave function renormalization for the diagrams of type (5) (Figs. 5c and d) we observe that one simply has to replace $C_\mu(p', p')$ of (A10) by $2C_{\mu\nu}$ and one finds from (A11) and (A9)

$$B^{(n')} + O^{(n')} = 0 \quad (A12)$$

which expresses the identical cancellation of the divergencies of Figs. 5c, d, and e.

It may be remarked that (A12) can be concluded from (A11) alone since the requirement of gauge invariance connects the fundamental single corner and double corner parts of the Hamiltonian (2), and a consistent charge renormalization procedure has to yield $(e+\delta e)^2$ in front of the latter if it yields $e+\delta e$ in front of the former. The above proof, however, is not based on the consistency of the charge renormalization procedure.[28]

APPENDIX II. ON THE ASYMPTOTIC BEHAVIOR OF PRIMITIVE DIVERGENT INTEGRALS

Consider a primitive divergent integral which involves an integration over a single internal momentum t only. Assume that auxiliary variables $x, y, \cdots$ are used to combine the denominators[5] of a single-corner diagram. The integral will be of the form

$$\int dxdy\cdots d_4tP_n(t, p^i)/[(t-\Sigma a_j p^j)^2 + b^2]^F, \quad (A13)$$

where F is the number of internal lines, n the number of corners, and $P_n(t, p^i)$ a polynomial of order n in t whose terms are of the form $(p^i)^{t+s}$ with $r+s \leqslant n$. The α_j are polynomials in $x, y, \cdots$ and b^2 is quadratic in all the p^i with coefficients which are polynomials in $x, y, \cdots$. If we use regulators we are permitted to shift the variable $t \to t + \Sigma\alpha_j p^j$. The result of the t integration will, for any of the p^i large, behave as $(p^i)^{n-2F+4}$. From (34c) and the fact that only diagrams with $n \geqslant E$ can diverge $n - 2F + 4 \leqslant 4 - E$. Comparison with (40) shows that (A13) diverges for large p^i at most as the t integration itself. The same result can be derived for integrals with more than one t integration. Therefore the convergent functions introduced in (50) behave asymptotically as follows: $S_c \sim O(1)$, $D_c \sim O(1)$, $L_{\mu c} \sim O(p)$, $O_{\mu\nu} \sim O(1)$, $M_c \sim O(1)$, where $O(1)$ may imply a logarithmic dependence. This justifies the interpretation as smearing-out functions [as given following Eq. (52)] and it proves that diagrams with effective lines and corners diverge in the same way as those with ordinary lines and corners.

[28] For spin $\frac{1}{2}$ such a proof to second order was first given by R. P. Feynman, reference 5, p. 778. Also for spin $\frac{1}{2}$ and based on the charge renormalization procedure a proof was given by J. C. Ward, Phys. Rev. **78**, 182 (1950).